Flexible Heat Pump Integration to Improve Sustainable Transition Toward 4th Generation District Heating

Mohamed Hany Abokersh [a], Kangkana Saikia [a], Luisa F. Cabeza [b], Dieter Boer [a], Manel Vallès [a] *

[a] Departament d'Enginyeria Mecànica, Universitat Rovira i Virgili, Av. Països Catalans 26, 43007 Tarragona, Spain

[b] GREiA Research Group, Universitat de Lleida, Pere de Cabrera s/n, 25001 Lleida, Spain

* *Corresponding author: manel.valles@urv.cat*

E-mail addresses: mohamed.abokersh@urv.cat (M.H. Abokersh),ikangkana.saikia@gmail.com (K. Saikia), dieter.boer@urv.cat (Dieter Boer), luisaf.cabeza@udl.cat (L.F. Cabeza)

Abstract

The movement toward the 4th generation district heating (4GDH) embraces a great opportunity to support the future smart energy development concept. However, its development calls for addressing technological and economic obstacles aligning with the need for a reformation of the energy market to ensure the quality of service. In this context, our paper presents a comprehensive analysis based on a multi-objective optimization framework incorporating an artificial neural network-based model for the possibility of integrating heat pump (HP) into solar assisted district heating system (SDHS) with seasonal thermal energy storage to support the sustainable transition toward 4GDH. The study evaluates the performance of the proposed system with the help of key performance indicators (KPI) related to the 4GDH characteristics and key stakeholders for possible market growth with consideration for the environmental benefits. The proposed analysis is applied to a small neighbourhood of 10 residential buildings located in Madrid (Spain) to investigate the optimal integration of HP under different control strategies into a SDHS. Inherent the SDHS operator perspective, the results reveal a significant improvement in the stabilization of the SDHS performance due to the HP integration where the solar field temperature never exceeds 80°C, and the seasonal storage tank (SST) temperature stands at 85.4°C. In addition, the share of solar energy stands above 86.1% with an efficiency of 73.9% for the SST, while the seasonal HP performance factor stands above 5.5 for all optimal scenarios. From the investor viewpoint, an energy price of 59.1 Euro/MWh can be achieved for the proposed system with a payback period of 26 years. Finally, from the policymaker perspective, along with the significant economic and sustainable improvement in the SDHS performance, a substantial environmental improvement of 82.5% is achieved when compared to the conventional boiler heating system. The proposed analysis reflects a great motivation for different stakeholders to propose this system as a path toward the 4GDH in the future district energy systems.

Keywords: Solar assist district heating system; Heat pump; Artificial Neural Network; Multi-objective optimization; Key performance indicators; 4th generation district heating

Graphical Abstract

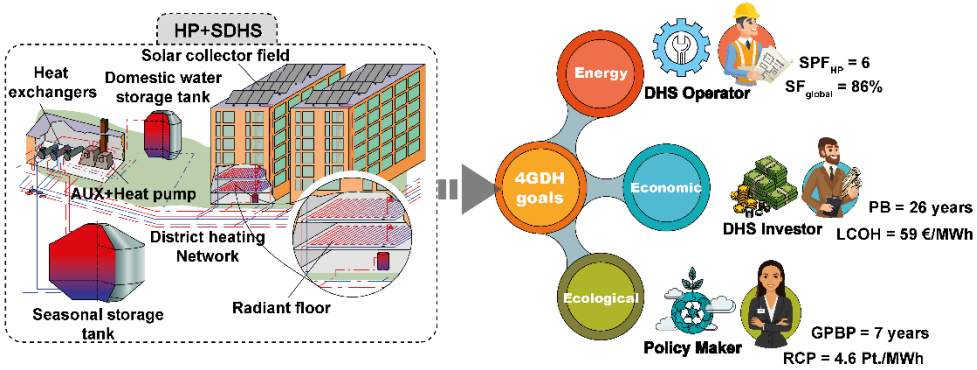

Highlights

- Framework to judge transition toward 4th generation district heating is proposed.
- Multi-objective optimization for evaluating heat pump effect is projected.
- Various control strategies for the heat pump operation are investigated.
- Stakeholder perspective is examined using KPIs of 4th generation district heating.
- Heat pump integration in district heating is a sustainable and competitive solution.

1 Nomenclature

A_{COL}	total aperture area of solar collectors (m²/(MWh·a))
β_{COL}	inclination angle of the solar collectors (°)
C_C	total initial capital cost (€)
C_O	total discounted operational cost (€)
C_R	total discounted replacement cost (€)
$Cap_{heating}$	heating capacity of the HP (MW)
d_{con}	construction material thickness of the seasonal storage tank (m)
d_{Roof}	insulation material thickness for the seasonal storage tank roof (m)
d_{Wall}	insulation material thickness for the seasonal storage tank wall (m)
d_{Gnd}	insulation material thickness for the seasonal storage tank ground (m)
DAM_d	indicator result for damage category d
DAM_{off}	Indicator for the environmental damage limits
FC_{AUX}	contribution of the auxiliary heater as a percentage of the maximum heating load (-)
$f_c(x)$	original objective function [$LCOH$(x) or RCP(x)]
FC_{HP}	fraction capacity of the heat pump (-)
$g(x)$	inequality constraints
$h(x)$	equality constraints
h_{conv}	convective heat transfer coefficient to the air W/(m²·K)
HDR	seasonal storage tank aspect ratio (m/m)
HDR_{DHWT}	domestic hot water storage aspect ratio (m/m)
k	number of regressors
$LCOH$	Levelized cost of heat (€/MWh)
$\dot{m}$	mass flowrate of the recirculating water pumps (kg/s)
n	sample size
N_{COL}	number of solar collectors in series
$\dot{P}_{heating}$	power drawn by the heat pump (MW)
$\dot{Q}_{SOL}$	useful energy rate received by the solar collector field (MW)
$\dot{Q}_{Useful}$	useful energy produced by the solar collector field (MW)
$\dot{Q}_{SST\ loss}$	heat loss rate through the seasonal storage tank (MW)
$\dot{Q}_{DHW\ loss}$	heat loss rate through the domestic hot water storage tank (MW)
$\dot{Q}_{HE}$	heat transfer rate through the heat exchanger (MW)
$\dot{Q}_{AUX}$	duty of auxiliary heater (MW)
$Q_{SH\ load}$	total space heating demand (MWh)
$Q_{DHWload}$	total domestic hot water demand (MWh)
$Q_{SST\ loss}$	total energy losses through the seasonal storage tank (MWh)
R	seasonal storage tank radius (m)

r	interest rate (%)
R_a	revenue of the system (€)
R^2-adj	adjusted coefficient of determination
RCP	ReCiPe 2016 aggregated impact factor (Pt/MWh)
SF_{DHW}	annual solar fraction for the DHW distribution circuit (%)
SF_{global}	overall solar fraction (%)
SF_{SH}	annual solar fraction for the SH distribution circuit (%)
SPF_{HP}	seasonal performance factor (SPF)of the heat pump
$T_{load,in}$	temperatures of the liquid entering on the load side (°C)
$T_{load,out}$	outlet temperatures of the load side (°C)
T_{Return}	return temperature of the district heating network (°C)
$T_{source,out}$	outlet temperatures of the source side (°C)
$T_{source,in}$	temperatures of the liquid entering on the source (°C)
T_{Supply}	supply temperature of the district heating network (°C)
$U_{Overall}$	overall heat loss coefficient of the seasonal storage tank (W/(m^2·K))
V_{DHWT}	volume of the domestic hot water tank (m^3/(MWh·a))
V_{SST}	volume of the seasonal storage tank (m^3/(MWh·a))
$y_{predict,i}$	predicted value
$y_{data,i}$	actual value

Greek symbols

η_{COL}	solar collector field efficiency (%)
η_{DHWT}	domestic hot water storage tank efficiency (%)
η_{SST}	efficiency of the seasonal storage tank
λ_{con}	construction material thermal conductivity of the seasonal storage tank (W/(m·K))
λ_{ins}	insulation material thermal conductivity for the seasonal storage tank roof and wall(W/(m·K))
λ_G	ground thermal conductivity (W/(m·K))
$\lambda_{ins\ gnd}$	insulation material thermal conductivity for the seasonal storage tank ground (W/(m·K))
δ_d	normalization factor for damage category d
ε_d	weighting factor for damage category d
ΔT_{SST}	temperature difference between the extracted and replaced water inside the space heating circuit
ΔT_{DHW}	temperature differences between the extracted and replaced water at storage tanks to cover the DHW load
ΔT_L	temperature difference between the exit and entrance of the auxiliary heater

Abbreviations

4GDH	4th Generation District Heating
ANN	Artificial Neural Network
AUX	Auxiliary Heater (fuelled by natural gas)

COL	solar collector field
DH	District Heating
DHW	Domestic Hot Water
DHWT	Domestic Hot Water Tank
FG	Foam Glass gravel
GA	Generic Algorithm
GPBP	Greenhouse gas payback period
HE	Heat Exchanger
HP	Heat Pump
HPC	High-Performance Concrete
KPI	Key Performance Index
LCA	Life Cycle Assessment
LCIA	Life Cycle Impact Assessment
MOO	Multi-Objective Optimization
MOGA	Multi-Objective Genetic Algorithm
MW	Mineral Wool
NC	Normal Concrete
P	Centrifugal pump
PB	Payback Period
SAHP	Solar Assisted Heat Pumps
SDHS	Solar Assisted District Heating System
SH	Space Heating
SST	Seasonal Storage Tank
STES	Seasonal Thermal Energy Storage
TES	Thermal Energy Storage
TRNSYS	Transient system simulation program
UHPC	Ultra-High-Performance Concrete
XPS	Extruded Polystyrene

Indices

d	damage category
i	elementary factor
k	equipment unit

1. Introduction

Energy infrastructure around the world is undergoing a transitional period to accommodate the highest possible share of renewable energy generation in the existing grid and provide reliable service to meet the demand in various sectors. With the revised EU directive on renewable energy, the European countries are focusing on delivering 32% of the total energy from renewable energy sources, such as wind, solar, and biomass, by the year 2030 [1]. In efforts to push this energy transition, the EU has also decided that beginning in 2021, the proportion of renewables in the heating/cooling sector will rise by 1.3% points annually. In this context, district heating (DH) networks have gained a great deal of attention with the possibility of integrating them into the future smart energy system.

The smart energy system concept is a broader definition of the smart grid moving the sole focus from the electrical power grid towards the integration of different energy sectors such as electricity, heating, cooling, industry, buildings, and transportation to achieve sustainable energy solutions [2]. In such a future energy vision, the district heating systems can play a crucial role by allowing the use of industrial waste heat and local renewables such as solar energy in combination with large scale thermal energy storage to transform into a low-temperature thermal grid which is also known as 4th generation district heating (4GDH) [3–6]. The 4GDH system has emerged as a promising technology because conventional high-temperature DH systems experience substantial heat losses and high installation costs [7] as well as the possibility of losing profit when the heating demand is decreased due to the renovation of existing buildings [8]. The key characteristic of 4GDH is considered to be the ability to deliver heat at a much lower temperature range (50 ~ 60°C) and significantly lowering the return temperature (25 ~ 30°C) [9],[10]. However, the implementation of a 4GDH needs further research in order to address technological and economic obstacles and reform the energy market framework to ensure the quality of service [11].

Different technologies can be combined with DH systems to improve efficiency and energy savings [12]. The large-scale solar thermal district heating plants are among the most interesting solutions that have already become a reality today in countries like Denmark, Sweden, Austria, Germany, Spain, and Greece [13], [14]. Such a system has the edge over the conventional heating system reducing the use of fossil fuels and emissions. Still, it deals with a higher degree of flexibility issues due to the fluctuating nature of solar radiation. The variation in heat load with changing seasons does not match with heat generation by the solar source creating an unfavourable condition for 4GDH [15]. This issue can be resolved by coupling seasonal thermal energy storage (STES) to solar thermal plants where the heat produced can be stored for later use [16]. Despite that, the solar heating system may fail to reach the expected level of solar fraction for seasonal storage (50-100%) and short term storage (10-20%) due to the high heating demand of the building, high return temperature to the storage, and high heat loss from thermal storage [17]. One way to reduce the storage heat loss is to maintain a low temperature inside the storage tank. Such control measures require a supporting device such as back up heat pumps for effective space heating (SH) [18]. With the aid of heat pumps, STES can be discharged to lower temperature levels, collectors under a low-temperature condition can reach higher solar fraction, and the whole system is less prone to fluctuating district heating network return temperature [19]. Heat pumps are also highly efficient when operated in low-temperature DH networks to supply temperatures below 70°C [20]. Therefore, introducing heat pumps into a solar assisted district heating with seasonal storage can be a promising technological intervention to improve the overall system efficiency and transform the existing plants into a 4GDH system [17] [21].

Heat pumps present low CO_2 emissions when used under high-efficiency conditions, in particular, the electrically powered heat pumps with electricity from renewable sources [22]. One way of using electric heat pumps for residential and commercial heating applications is to combine the technology with solar systems, i.e., solar thermal, solar photovoltaic [23], or both thermal and photovoltaic (PV/T) [24]. During recent years, a variety of solar-assisted heat pumps (SAHP) configurations are proposed and analyzed for

the water heating application. Standard SAHP concepts such as direct expansion [25] and indirect expansion style [26] along with modified novel design such as SAHP with hybrid solar collectors [27], dual tank SAHP [28] have been investigated to show their feasibility from economy and energy conservation perspective. Concerning the integration of heat pumps into district heating networks, Kim et al. [29] designed a TRNSYS model consisting of a solar thermal system, seasonal storage, high temperature and low-temperature heat pumps which showed significant energy savings when the solar fraction is increased by varying the size of collectors and storage. Østergaard and Andersen [30] in another study assessed the potential of booster heat pumps to provide domestic hot water demand in a low-temperature district heating scheme. Hirvonen et al. [31] examined the influence of community size on the technical as well as the economic performance of a solar assisted district heating and a ground source heat pump for additional heat generation. Another optimization study compared a heat pump integrated centralized solar district heating with a semi-decentralized one and found that the decentralized system outperforms the centralized system in terms of life cycle cost [32]. These studies highlight that heat pumps can add more flexibility to the district heating network either by directly supplying SH and domestic hot water (DHW) load or charging up the storage tank. This allows shifting the use of electricity and reducing natural gas consumption, which leads to improved energy security.

The simulation-optimization studies on solar assisted district heating systems (SDHS) with storage and heat pumps are so far primarily focused on analyzing parameters associated with the solar source, storage technology, and energy demand profile of the community from the techno-economic point of view. However, efforts towards designing the whole SDHS framework to an optimal extent from the sustainability standpoint while fulfilling the targets of next-generation district heating are seldom found [33,34]. More importantly, the possible role that heat pumps can play in a SDHS network to address the issues related to storage heat loss and overall flexibility of the network has not been fully explored. This aspect of heat pump utilization to maintain an efficient low-temperature SDHS network may lead to high initial investment, electricity consumption, and related CO_2 emission. Hence, the optimization of the key design parameters of heat pump integrated SDHS becomes more important. It should consider energy efficiency, economic feasibility, and environmental impact simultaneously to ensure that such a system is walking hand in hand with the sustainable development goal. Nevertheless, such an optimization problem is complex enough to solve and takes more computational resources to take multiple decision variables into account within the same framework. Therefore, we are introducing a meta-modeling method in this study to minimize computational effort while maintaining high accuracy rates.

The Artificial Neural Network (ANN) is one of the most widely used meta-model techniques for dealing with complex design problems in energy research compared to traditional algorithms when managing a large data set [35], [36]. ANN can find a relation between the input and output variables by studying previously recorded data and reproduce a comprehensive model based on that relationship [37]. In order to demonstrate the applicability of ANN, Esen et al. [38] used the backpropagation learning algorithm to predict the coefficient of performance of a horizontal ground-coupled heat pump system. Xia et al. [39] devised an ANN model using genetic algorithms to perform multi-objective optimization of a SDHS. Another proof of concept was developed by Hirvonen et al. [40], where neural network meta-modeling is used to optimize a solar community to supply the heating demand, and the proposed method provided better solutions compared to genetic algorithms.

This paper aims to analyze the techno-economic performance as well as the environmental impact of different control strategies for integrating heat pumps into SDHS equipped with seasonal thermal energy storage in the context of 4GDH. Emphasis is given mostly on district heating consumption for SH with less focus on DHW consumption. Two types of control strategy are proposed where the heat pump is connected in series with the solar collector. Each control concept is investigated through dynamic simulations in TRNSYS and multi-objective optimization based on an ANN model to determine the optimized combination

of key design parameters based on energy performance, economic, and environmental impact. The results are used in a comparison of the seasonal storage enhanced SDHS with and without the inclusion of heat pumps. Furthermore, the study evaluates the performance of the proposed system with the help of key performance indicators (KPI) related to the 4GDH characteristics and key stakeholders for possible market growth and expansion.

Hence, the novelty of the work is to demonstrate the potential of heat pump integration into a community sized SDHS to stabilize its performance and assist in the sustainable transition towards 4GDH. Another novelty of this paper is the development of optimized control strategies for the heat pump operation to enhance the overall flexibility of the SDHS. The presented research, therefore, lays the groundwork for stakeholders of a SDHS with seasonal storage and heat pumps to navigate the next generation district heating transformation.

The structure of the article is as follows: A general outline of the SDHS and its mathematical definition is proposed in section 2. In section 3, both the techno-economic targets and environmental aspects are explained in terms of KPIs based on the stakeholder perspective. The design of an ANN-based optimization strategy is introduced in section 4. Section 5 discusses the deployment of methodology in a community of 10 residential buildings in Madrid, Spain, and section 6 provides the relevant findings and discussions. The results of the study are eventually summarized in section 7.

2. System description and simulation

2.1. System development

A distinct typology of heat pump integrated into SDHS is designed to meet the space heating and domestic hot water demands for a hypothetical residential neighbourhood throughout the year as schematically shown in Fig. *1*. The system mainly consists of solar collectors, a half-buried sensible seasonal storage tank (SST), the DHW storage tank (DHWT), a water-to-water heat pump unit, and auxiliary natural gas heaters.

The heat pump (HP) acts as a heat source for the SST when connected in the solar field circuit, as shown in Fig. *1*. In this configuration, the heat captured by the solar collector field (COL) can be directly used to fulfill the SH or DHW demand of the district or stored in the SST. The heat exchangers transfer the heat from the supply circuit to the distribution network using Y-type valves, depending on the mode of operation. Under a certain condition, the heat produced by the HP is either distributed directly for space heating or supplied to the SST for charging up the heat stored. The SST is used during the winter season to supply the SH demand, while the short-term storage DHWT is used to supply the daily DHW demand. It is important to note here that the heat provided for SH corresponds to a low-temperature level (50°C), whereas the heat provided to the DHW is at high-temperature level (60°C). Finally, if the solar field, SST, and HP fail to meet the heat demand, the mismatch is covered by the auxiliary heater.

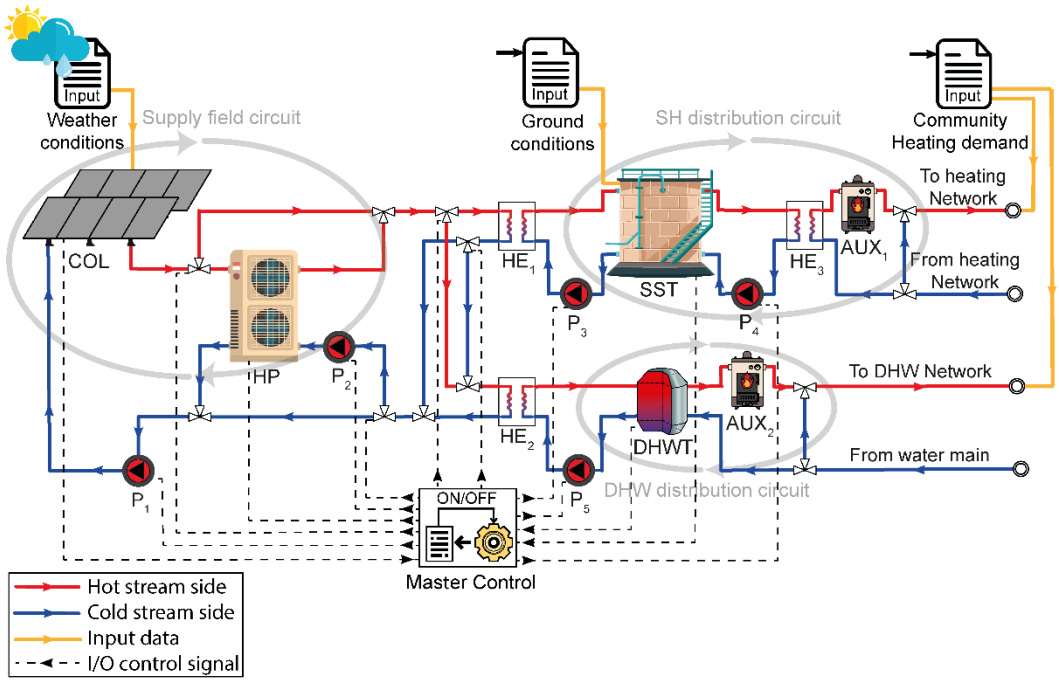

Fig. 1: A schematic drawing for the HP integrated with SDHS.

2.2. Control logic

The developed system requires a good control strategy to operate under different modes to meet the district heating demand while maximizing the solar fraction and minimizing the heat losses. Four modes of control are designed based on the temperature levels at different points of SDHS, and these are achieved through on-off control of the isolation valves.

At first, when the DHW mode is triggered on, the heat gained by the solar collectors is transferred to the DHWT with the aid of the centrifugal pumps P_1, P_2 and P_5 via HE_2. The auxiliary heater is only enabled when the solar heat is not adequate to cover the demand in the DHW network. Under DHW mode, the heat pump unit is non-operational.

The SH mode is activated when an appropriate value of the temperature in the DHWT is reached, and the COL temperature is at a higher level than the bottom temperature of the SST. This operating mode uses the pumps P_1, P_2 and P_3 to deliver the heat to the SST from the solar collectors passing through the heat exchanger HE_1.

The third mode of control is for the simultaneous operation of DHW and SH circuits. This is activated only when the conditions for both DHW and SH operation are achieved, and the temperature in SST is higher than the DHWT.

Finally, the heat pump operation has two activated modes:

- *Control (A)* — In this mode, the heat pump works when the mean SST temperature (T_{SST}) is less than a reference temperature (T_{ref}).
- *Control (B)* — In this mode, the heat pump works if the solar collector temperature (T_{COL}) is less than the mean SST temperature (T_{SST}), which is, in turn, less than a reference temperature (T_{ref}).

In these modes of operation, the heat generated by the heat pump in Control (A) & (B) will be transferred either to the SST or the DHWT based on the demand. In case of insufficient supply from SST or DHWT, the auxiliary heater is turned on.

2.3. System modeling

The concept is modeled using standard modules available on TRNSYS 18 environment based on the previous works by Tulus et al. [41], and Abokersh et al. [42]. Simulations are carried out for model training and performance assessment of the developed model. The major components of the TRNSYS model are explained in SI 1.

The SDHS model in TRNSYS is simulated considering a time step of 15 minutes. The simulations are carried out for a timeframe of three years, and the corresponding results are then extrapolated throughout the SDHS lifetime. This criterion is based on the assumption that the temperature within the SST remains at 30°C in the first year, and only after two years of simulation, the effect of the temperature change becomes negligible for the following years [43]. The lifetime of the SDHS is considered to be 40 years as set by the United Nations Environment Programme [44]. Replacements are required for the equipment such as the solar collectors, heat pump, heat exchangers, DHWT, auxiliary heaters, and centrifugal pumps after continuous operation for 20 years.

3. Evaluation of System Performance

To evaluate the performance of the proposed heat pump integrated SDHS, a set of performance indicators was selected. The set includes indicators to provide information on energy efficiency as well as the economic and environmental performance over the entire lifetime of the system.

3.1. Energy performance indicators

The energy evaluation indicators comprise of the efficiencies of the solar collector, SST, and DHWT [45], [46], seasonal performance factor (SPF) of the heat pump [47], and the overall solar fraction of the SDHS [48], [49]. The analysis is carried out using the following Eqs. (1) to (5) where the indicators are expressed in terms of the amount of energy flowing in the corresponding equipment unit:

$$\eta_{COL} = \frac{\int_0^t \dot{Q}_{Useful}}{\int_0^t \dot{Q}_{SOL}} \tag{1}$$

$$\eta_{SST} = 1 - \frac{\int_0^t \dot{Q}_{SST\ loss}}{\int_0^t \dot{Q}_{HE_1}} \tag{2}$$

$$\eta_{DHWT} = 1 - \frac{\int_0^t \dot{Q}_{DHW\ loss}}{\int_0^t \dot{Q}_{HE_2}} \tag{3}$$

$$SPF_{HP} = \frac{\int_0^t Cap_{heating}}{\int_0^t \dot{P}_{heating}} \tag{4}$$

$$SF_{global} = 1 - \frac{\int_0^t Cap_{heating} + \int_0^t \dot{Q}_{AUX_1} + \int_0^t \dot{Q}_{AUX_2}}{Q_{SH\ load} + Q_{DHW\ load}} \tag{5}$$

where $\dot{Q}_{Useful}$ and $\dot{Q}_{SOL}$ are the useful solar energy produced and received by the solar collectors, respectively. The heat losses in the SST and DHWT are represented by $\dot{Q}_{SST\ loss}$ and $\dot{Q}_{DHW\ loss}$, while the

rates of heat transfer through the heat exchangers HE_1 and HE_2 are given by $\dot{Q}_{HE_1}$ and $\dot{Q}_{HE_2}$. Moreover, $\dot{Q}_{AUX_1}$ and $\dot{Q}_{AUX_2}$ are the energy provided by the auxiliary heaters to supply the SH load ($Q_{SH\ load}$) and DHW load ($Q_{DHWload}$) under the condition of insufficient solar energy.

3.2. Economic parameters

The Levelized cost of heat ($LCOH$) is adopted in our study for evaluating the economic competitiveness of the proposed SDHS, as demonstrated by Welsch et al. [50]. $LCOH$ in EUR per MWh is the minimum price at which the SDHS must supply heat to the customers at a pre-defined maximum temperature of the working fluid [51]. The $LCOH$ is performed by dividing the total discounted life cycle cost of the SDHS by the discounted thermal energy output Q_a of the SDHS as shown by the following formula [52]:

$$LCOH = \frac{\sum_{N=0}^{N_{end}} (C_C + C_O + C_R - R_a).(1+r)^{-N}}{\sum_{N=0}^{N_{end}} Q_a (1+r)^{-N}} \quad (6)$$

Here $LCOH$ evaluation takes place over the assumed valuation period from $N = 0$ to N_{end} which takes into account of all costs associated with the SHDS during its lifespan, i.e., initial investment (C_C), operations and maintenance cost (C_O), equipment replacement cost (C_R) and the revenue of the system (R_a). An interest rate r is assumed. The $LCOH$ analysis requires all cost components to be converted into their present value. The revenue of the system (R_a) is not considered in this calculation. The details regarding the $LCOH$ components and their respective calculations can be found in SI 2. In addition, the economic parameters for the initial cost and other life cycle cost inputs are mentioned in SI 3.

Another most commonly used cost-analysis methodology is the payback period (PB), which determines the number of years required to recover an initial investment through economic returns of the project. Therefore, the payback period of our proposed SDHS is the ratio of the total life cycle cost of the SDHS to the annual cost savings due to using SDHS instead of natural gas, as shown below [53]:

$$PB = \frac{LCOH}{Annual\ cost\ saving} \quad (7)$$

3.3. Environmental assessment

For addressing the environmental impacts of coupling heat pumps with the SHDS system and comparing it with those of different district heating technologies, a life cycle assessment (LCA) approach is used [54]. The life cycle impact assessment (LCIA) can be performed using a variety of impact indicators. In this study, we follow the framework ReCiPe 2016 [55], which is considered as the most adaptable and uniform approach from a methodological point of view [56]. In this phase, the Life Cycle Inventory data are converted to endpoint impact indicators, which are again combined to represent three damage categories: human health, ecological systems, and resources. Afterwards, the three damages are aggregated and expressed as a normalized endpoint indicator metric (RCP) to interpret the overall environmental performance of the proposed SDHS configuration. The RCP can be expressed, as shown below:

$$RCP = \sum_{d} \delta_d \varepsilon_f DAM_d \qquad \forall d \quad (8)$$

Here DAM_d is the endpoint impact indicator for the damage category d. δ_d is the normalization factor based on land use and material extraction for the European setting while the weighting factor ε_d is based on recommended values by ReCiPe 2016. The environmental impact of SDHS components is found in SI 3.

Additionally, the greenhouse gas payback period ($GPBP$) is introduced to estimate the sustainability of the proposed SDHS model [57]. The GPBP is the number of years of operation taken by the renewable energy plant until the total GHG savings due to the replacement of fossil energy by renewable energy equals the GHG emissions during the life cycle [58]. It represents the potential of the SDHS model to reduce the environmental impact, and can be expressed as follows:

$$GPBP = \frac{RCP}{Annual\ RCP\ saving} \tag{9}$$

3.4. Key performance indicators (KPI) for successful 4GDH implementation

In the previous section, several performance indicators are described not only to evaluate the specific energy, economic and environmental characteristics of the proposed HP+SDHS but also to provide an appropriate identification of margins by which the system intends to meet the criteria of 4GDH concept. For this purpose, performance indicators that would demonstrate a successful representation of a specific target of 4GDH are used as KPIs in the current study and defined as shown in Table 1.

Table 1: Key performance indicators for DHS transition evaluation based on the 4th generation goals.

KPI	**Symbol**	**Unit**	**4th generation goal**
KPI$_1$ — Share of renewable energy (solar)	-	%	Up to 100%
KPI$_2$ — Seasonal Performance factor of the heat pump	SPF_{HP}	-	> 2.5[47]
KPI$_3$— District heating supply and return temperatures	T_{Supply}, T_{Return}	^{o}C	50, 25
KPI$_4$ — Thermal efficiency of the SST	η_{SST}	%	Up to 100%
KPI$_5$ — Temperature level of the solar collector field	T_{COL}	^{o}C	< 100 ^{o}C
KPI$_6$ — Temperature level inside the SST	T_{SST}	^{o}C	< 80 ^{o}C
KPI$_7$ — Levelized cost of heat	$LCOH$	€ /MWh	< Natural gas boiler cost
KPI$_8$ — Payback period	PB	Years	< 40 years
KPI$_9$ — Recipe impact indicator	RCP	Pt./MWh	< Natural gas boiler impact
KPI$_{10}$ — Greenhouse gas payback period	$GPBP$	Years	< 40 years

In order to attract the investors with environmental drivers as well the DHS operators, the KPIs are associated to the stakeholders' perspectives [59]. Guidelines from [11] and [60] on the 4GDH concept have helped to select appropriate efficiency and sustainability indicators that complete a comprehensive assessment of the targeted solutions. Fig. 2 summaries the proposed KPIs for respective stakeholders and their justification in a heat pump integrated SDHS.

Fig. 2: The 4GDH goals from the stakeholders' perspective connected to the KPIs.

4. Development of design optimization strategy

4.1. Outline for optimization approach

The main objective of the optimization approach is to minimize the life cycle cost ($LCOH$) simultaneously with the environmental impact (RCP) of the heat pump integrated into the SDHS. The outline of the optimization strategy is illustrated in Fig. 3. This approach is developed based on the TRNSYS model mentioned in section 2. Once the TRNSYS model is built, we define the decision variables' range in the optimization problem, which, if changes reflect in the thermal output of the TRNSYS model. The software MATLAB is utilized to create the required scenarios where these scenarios cover the feasible range for the decision variables. Following that, MATLAB runs the scenarios automatically through TRNSYS in a parallel way. Once the feasible scenarios are built, the ANN model is trained using the developed scenarios in order to predict the thermal performance of the SDHS. Finally, a genetic algorithm (GA) is coupled with the ANN to formulate a multi-objective optimization problem with an objective to minimize the cost functions aligning with the optimization problem constraints.

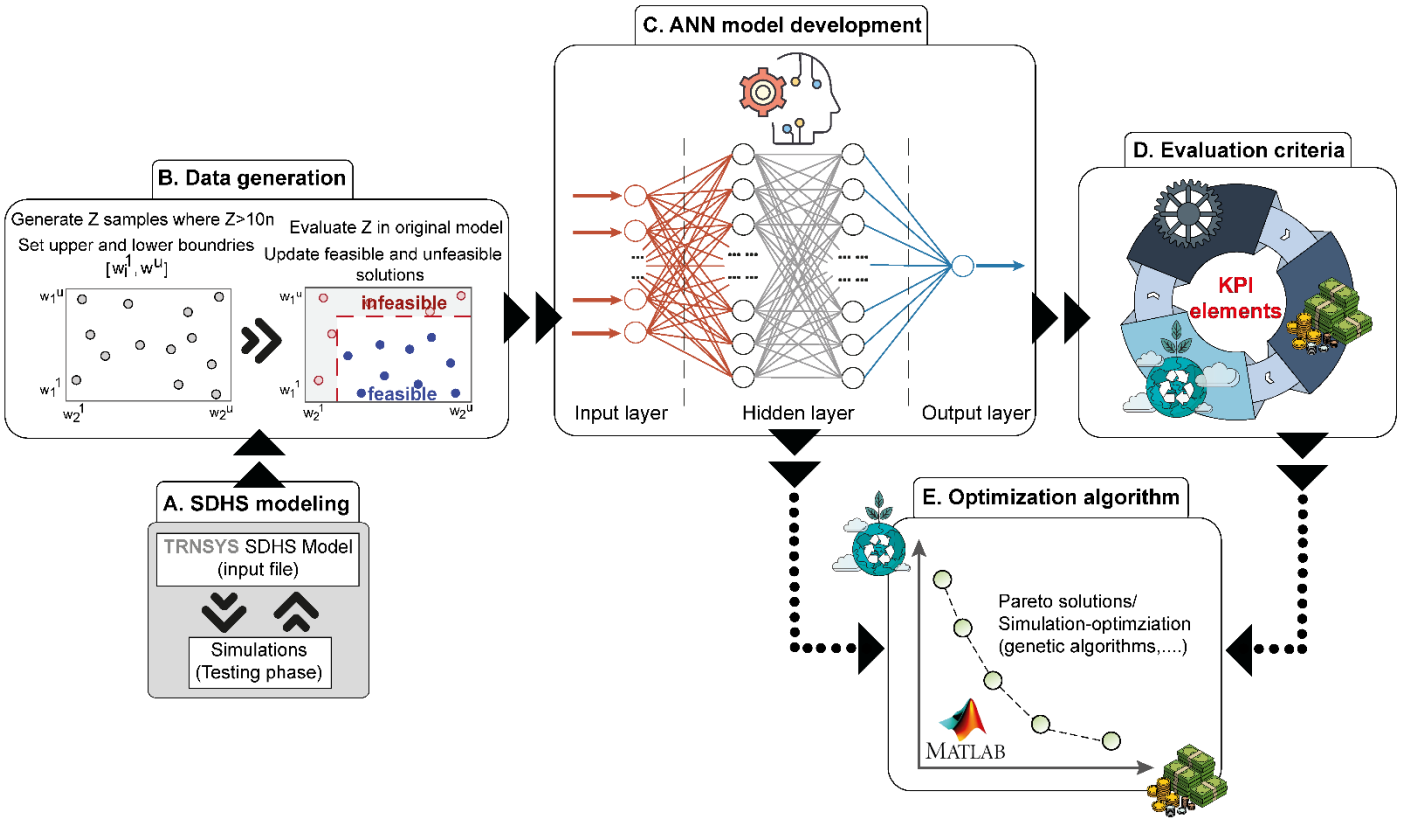

Fig. 3: The optimization strategy outline.

4.2. Development of the ANN performance model

4.2.1. Data generation

The metamodel approach begins by generating an initial set of samples to train the metamodel. Aligning with the size of the decision variables and the computational budget, an appropriate size of the initial samples is selected. After that, the metamodel is trained using 2048 samples based on the Abokersh et al. [42] recommendation. In our framework, we apply the low-discrepancy sequences (Sobol's LP_T) for sampling due to its good space-filling feature [61]. The TRNSYS simulations are then evaluated based on the generated samples where the feasible solutions are utilized for training the metamodel, and the infeasible solutions are discarded.

4.2.2. ANN model convergence criteria

The metamodel is built based on a multi-layer feedforward ANN model, where this model contains 14 neurons in the input layer and three hidden layers. The ANN simulations are implemented based on the Bayesian regularization algorithm with a learning rate, and a Momentum mean of 0.001 and 0.004. The model structure is determined through the optimization approach proposed by Abokersh et al. [42] to provide a relatively good convergence. In the ANN model, 19 outputs are considered in the output layer. These outputs include the energy produced in the solar collector field, the energy supplied by the heat pumps, the energy supplied by the storage tanks, and finally, energy covered by the auxiliary heaters. To verify the performance of the metamodel, a set of performance metrics are proposed to assess the

metamodel accuracy. These performance metrics are; (i) adjusted R-squared (R^2–$adj.$), and (ii) Coefficient of Variation ($C.V$), and they are estimated as shown in the Eqs. (10) to (12):

$$R^2 = 1 - \frac{\sum_{i=1}^{n}\left(y_{predict,i} - y_{data,i}\right)^2}{\sum_{i=1}^{n}\left(y_{data,i} - \overline{y}_{data}\right)^2} \tag{10}$$

$$R^2 - Adj. = 1 - \frac{(1 - R^2)(n-1)}{n-k-1} \tag{11}$$

$$C.V(\%) = \sqrt{\frac{\sum_{i=1}^{n}\left(y_{predict,i} - y_{data,i}\right)^2}{\overline{y}_{data}}} \times 100 \tag{12}$$

Where $y_{predict,i}$ presents the estimated value at time point i, $y_{data,i}$ is the actual value at time point i, n is the size sample, and k is the number of regressors.

4.3. Multi-objective optimization

In the formulation of the SDHS optimization problems, the cost functions usually create concerns about the energy performance and the economic profits [43]. However, in real problems, the environmental impact should be considered in the optimization framework to reflect the policy decision-makers' perspective. Therefore, our optimization problem tends to minimize the life cycle cost of the SDHS ($LCOH$) aligning with the environmental impact presented by the RCP to satisfy certain technical constraints. It is given as:

$$\begin{aligned} &min\ \{f_1(x), f_2(x)\} \\ &s.t.\ h(x) = 0 \\ &\quad g(x) \geq 0 \\ &lb_i \leq x_i \leq ub_i \qquad i \in \{1, \dots, 17\} \end{aligned} \tag{13}$$

Where f_1 is the life cycle cost ($LCOH$) and f_2 is environmental impact aggregated by ReCiPe 2016 (RCP), while h represents the equality constraints solved implicitly in TRNSYS. The symbol $g$represents the inequality constraints, which reflects certain technical constraints comprising an annual solar collector field efficiency of 60%, SST efficiency above 50%, and global solar fraction of 50%, as mentioned by Bauer et al. [62] and Solites [63].

In the current study, we utilized a Multi-Objective Genetic Algorithm (MOGA) [64] due to its capability to be coupled with metamodels easily [65]. In particular, the MOGA has the ability to handle several sets of Pareto points simultaneously. These sets of points are known as individuals in a population. Similar to the evolutionary algorithm, the initial populations can be modified with the proceedings of the iterations. These populations are generated with the application of the mutation and crossover functions [66]. The process is following the internal ranking of the population. For the available number of individuals in the population and iterates, the optimization is performed by evaluating the fitness function. The process is continued unless the criteria of convergence are met. All the information that is required for the evaluation of the sustainability metrics is available in the fitness function. The values of the fitness function for every sample point are used for the construction of the metamodel. Finally, the constraints associated with the metamodel simulator are handled through a penalty function [67]. A summary of the MOGA procedure is shown in Fig. 4.

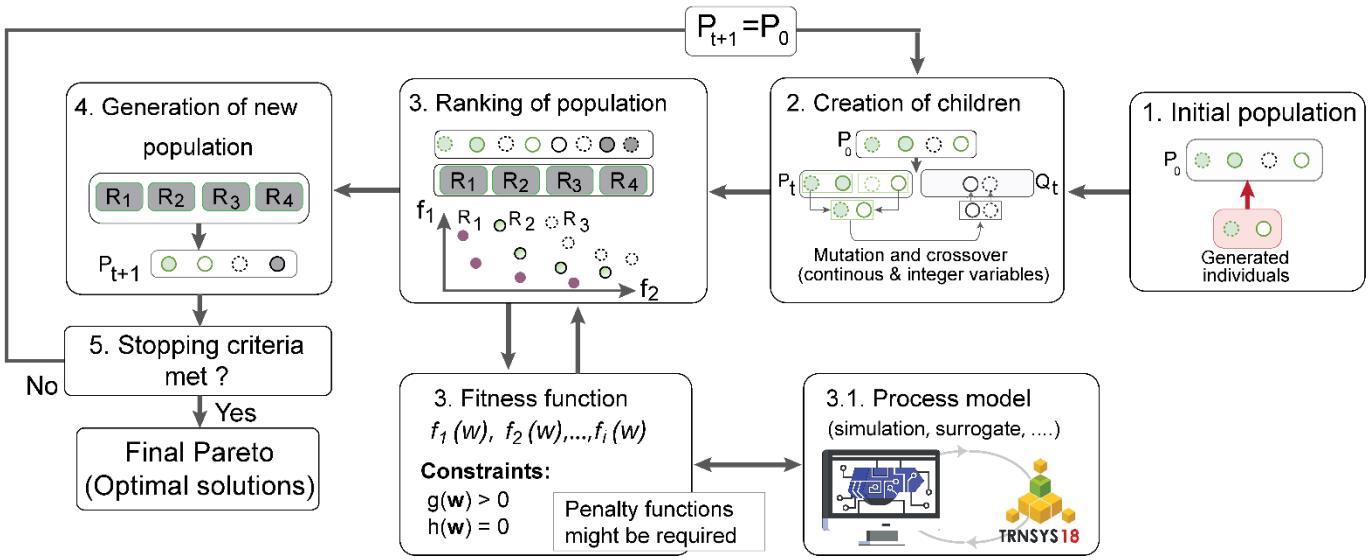

Fig. 4: Flow diagram for the MOGA and TRNSYS simulations.

4.4. Decision variables

In the current study, 17 decision variables are used in the formulation of the SDHS optimization problem. Different components of the SDHS comprising their relative orientation, construction, operational conditions, and sizing are included on the basis of these decision variables. The circuit name is used for the categorization of these decision variables. The decision variables in the supply field circuit comprise the solar collector field, its relative orientation, and the heat pump capacity with consideration for its operation criteria. In the SH distribution circuit, the SST and its relative construction materials are considered as decision variables in addition to the required auxiliary heater capacity in this circuit. In the DHW field, the DHWT volume and its relative construction ratio are considered aligning with the required auxiliary heater capacity in this circuit. A summary of these decision variables and their relative range is shown in Fig. 5. Furthermore, the sizing of other SDHS equipment is estimated based on mathematical equations linked with the decision variables.

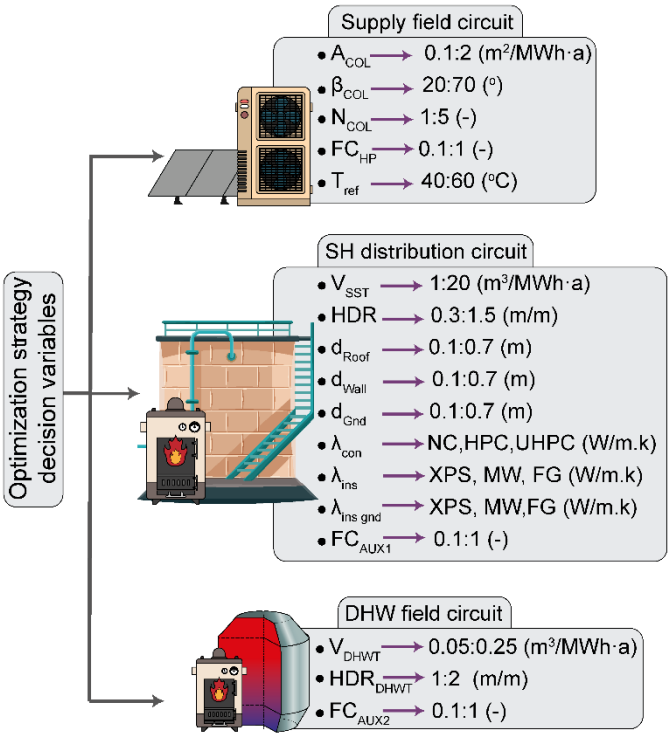

Fig. 5: SDHS optimization decision variables.

5. Case study

5.1. Description

A small urban neighbourhood of 10 buildings located in Madrid (Spain) is utilized to illustrate the rule of the heat pump in enhancing the sustainable performance of SDHS under different control strategies. In the proposed community, every building consists of seven floors with 28 apartments where each one has a 90 square meter of a functional area [68]. The apartments are facilitated with a radiant underfloor heating and domestic hot water system. Therefore, the proposed system is designed to cover the SH and DHW demands at 50°C and 60°C, respectively. The comparison of the SDHS heating demand and model validation was carried out based on Tulus et al. [41].

To carry out a comparative study and showcase the benefits of the proposed configurations, two reference cases are also considered; a district heating system fueled by natural gas (baseline 1) and a SDHS without integrated heat pumps (Baseline 2) as reported by Abokersh et al. [42].

5.2. Meteorological data and energy demand profiles

The EnergyPlus database [69] is utilized to acquire the required climatic data for Madrid. These data comprise the incident solar radiation and the ambient temperature. The monthly average values for these climatic data are shown in Fig. 6.

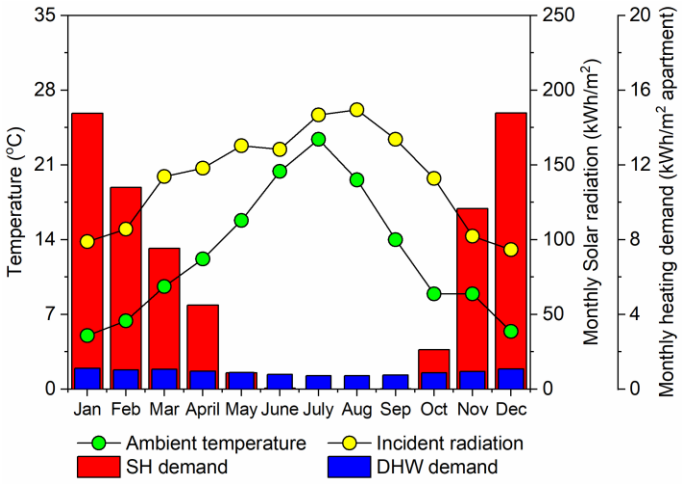

Fig. 6: The monthly climate conditions as well the SH and DHW demand profile of the investigated neighbourhood located in Madrid.

Based on the Spanish regulation for residential buildings, a seven floor building is simulated in the TRNSYS with consideration for the occupancy densities and the building material composition. The annual space heating demand profile is created based on the building simulation in TRNSYS following the work implemented by Guadalfajara [70]. The created space heating demand is then extrapolated for the whole neighbourhood where the total annual space heating for the neighbour is 1638.8 MWh. On the contrary, the DHW demand is generated based on DHWcalc [71]. This software generates representative DHW hourly demand profiles based on the daily water consumption per person and the number of occupants per household where the total annual DHW demand is 274.9 MWh for the specified neighbourhood. The monthly SH and DHW demands per apartment are shown in Fig. 6, where the total neighbourhood demand is 1638.8 MWh for space heating and 274.9 MWh for the DHW.

6. Results and discussion

In this study, the first part of the results offers an analysis of the ANN model to ensure the suitability of the metamodel for SDHS optimization. In the second part, the results obtained from the design optimization of the heat pump control strategy for integration with SDHS are presented via selected techno-economic and environmental performance indicators. A detailed analysis of the Pareto optimal solutions and the comparison between the results is carried out in this section. The third section provides a comparative study of the SDHS with and without HP to examine the possible effects of incorporating HP into SDHS for a small community. In the final stage of analysis, the capability of the developed system configuration is discussed in terms of the rate of achievements of 4GDH targets.

6.1. The ANN performance analysis

In the current study, the overfitting problem associate with the ANN model is solved through K-fold cross-validation, where the 2048 sample is divided into k subsets. Each time the ANN model is trained by k-1 set, whereas the remaining k subset is utilized for testing.

A summary of the ANN model performance is shown in Table 2. The results showed that the ANN model prediction is agreed with the TRNSYS output where the $R^2 - Adj.$ never falls below 95.5%for all the output. To gather further confidence regarding the ANN model performance, the $C.V$ shows that model accuracy does not get below 8.83% for all ANN output. In general, these results indicate the ability of the ANN model to provide an acceptable prediction for the thermal performance of the SDHS within the training data range.

Furthermore, the usage of metamodeling can offer a significant reduction in the computational expenses of heuristic optimization models.

Table 2: The performance sample of ANN model in predicting the TRNSYS output.

	Supply circuit				SH circuit			DHW circuit		
	Q_{SOL}	Q_{Useful}	Q_{abs}	P_{elec}	Q_{SST}	$Q_{SST\ loss}$	Q_{AUX1}	Q_{DHW}	$Q_{DHW\ loss}$	Q_{AUX2}
$R^2 - Adj.$	99.8%	99.6%	97.7%	97.8%	99.5%	97.7%	99.2%	95.5%	98.9%	99.4%
$C.V$	1.98%	1.99%	8.83%	8.16%	2.87%	8.54%	8.15%	0.49%	2.70%	3.08%

6.2. The effect of HP control strategy on SDHS

From the results viewpoint, the multi-objective optimization procedure is devoted to analyze the effect of the decision variables on the design of SDHS with heat pump under the two designed control systems A and B. The set of Pareto optimal solutions obtained from optimization process correspond to five scenarios. Scenario 1 represents the minimum cost solution with zero limits on possible environmental damage. The environmental damage limit of 25%, 50%, and 75% is allowed in scenario 2 up to 4 relative to scenario 1. In scenario 5, the SDHS model causes minimum environmental impact when 100% of the damage limit is hit.

It can be remarked from Fig. 7 (a) that a clear trade-off exists between the proposed economic and environmental targets as we switch from scenario 1 to 5 under both control settings. The optimal cost of energy in terms of $LCOH$ is increased while the environmental impact of the SDHS (RCP) is minimized and vice versa. The baseline 1 represents a traditional heating system (natural gas boiler). It produces the maximum environmental impact of 26.6 Pt/MWh as well as a limited economic benefit (90.3 €/MWh) compared to the Pareto optimal system configurations.

Under the control scheme (A), where the HP in SDHS is turned on if $T_{SST}$is less than the reference temperature; it can extensively minimize the environmental impact compared to the baseline 1 while remaining to be cost-competitive at scenarios 1 and 2. The optimal Min. cost solution has $LCOH$ equal to 72.1 €/MWh, which is less than the base case by 20.1%, whereas the RCP reduces to 5.15 Pt/MWh, which is smaller than the baseline 1 solution by 80.6%. On the other hand, the Pareto optimal solutions from scenarios 3 to 5 could not provide any economic benefit, although they minimize the environmental impact by approximately 89.5% compared to baseline 1.

Under the control setting (B), more enhancements of both objective functions can be seen compared to the Pareto optimal solutions under control (A) as well as in baseline 1. This is due to the efficient control of the heat pump with respect to temperature levels in the solar collector and SST, as well as the reference temperature. In scenarios 1 and 2, the $LCOH$ with control setting (B) is remarkably less than that of control setting (A) along with marginal environmental benefits. At control setting (B), the Min. cost solution has $LCOH$ equal to 59.1 €/MWh which is less than (A) by 18% and base case by 34.5%, whereas the RCP value is reduced to 4.65 Pt/MWh which is smaller than the solution (A) by 9.7% and the base case by 82.5%. As the environmental damage limits are increased from scenarios 3 to 5 with control setting (B) in action, the decreasing environmental impact leads to an increment in the cost. If the Min. impact solutions are compared, control (B) has the upper hand over (A) with significant cost reduction as it is reduced by 28.9%. However, this optimal solution still fails to beat the baseline 1 economically where it higher than the baseline 1 by 40.6%.

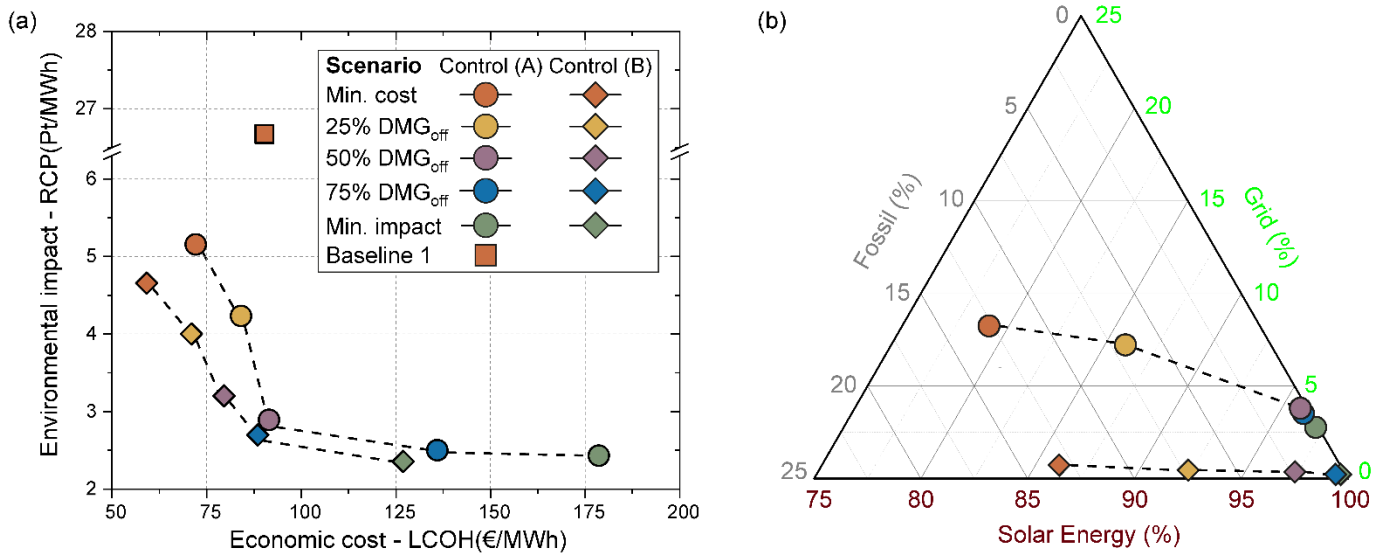

Fig. 7: Various Pareto optimal solutions for the HP integrated with SDHS under two control strategies (A) and (B) to cover the SH and DHW yearly demand in comparison to their respective baseline 1 using natural gas, (a) Levelized cost of energy and environmental impact of the optimal configurations at the different scenarios, (b) Energy source and its share for the optimal system configurations for the different scenarios.

Since the proposed SDHS system comes with multiple energy sources to optimize the environmental and economic parameters, the share of different energy sources is an important aspect to ascertain the system's feasibility as a future 4GDH system. The ternary representation of energy shares in Fig. 7(b) shows that as the Pareto front under the two control strategies (A) and (B) progress from generating the Min. cost-optimal solution to Min. impact, the SDHS can approach 100% solar energy input. For example, if the minimum cost solutions are compared, the Pareto optimal point under control (A) has 79.1% share of solar energy, 12.9% share of natural gas, and 7.98% share of grid electricity. Meanwhile, under control B, the optimal solution has 86.1% of solar energy, 13.1% share of fossil energy, and 0.73% share of grid proving that control mechanism (B) is more effective than (A). Regarding the rest of the scenarios (2-5), the share of solar energy in the system increases while the share of natural gas goes down when we move towards the minimum environmental impact solution. The control scheme (B) seems to be more successful with less percentage of electricity input from the grid for all the Pareto optimal solutions, and it reduces up to 3.5% and 0.3% for control (A) and (B), respectively.

In order to enhance the understanding of the system performance, a breakdown is conducted for each Pareto optimal solution under both control strategies (A) and (B). In Fig. 8, the optimal values for each decision variable are presented in a heat map in order to visualize how each design parameter changes under different optimization scenarios. Starting from the supply aspect, the design parameters related to the solar collector take similar values without any significant deviations except for the minimum cost scenario. In this case, the solar collector area decreases from 0.70 m^2/(MWh·a) under control (A) to 0.48 m^2/(MWh·a) under control (B). Similarly, the fractional capacity of the heat pump is significantly reduced under control (B), where the HP fraction is only 0.14±0.025 compared to 0.51±0.025 for control (A). This is expected since the heat pump is being operated only to stabilize the system, and it has a limited contribution to fulfill the thermal energy demand. Furthermore, the heat pump operation under control (A) keeps the reference operation temperature of the heat pump (T_{ref}) around 53.3±0.5°C for all optimal scenarios. While operating under control (B), the T_{ref} reduces from 55°C at the Min. cost solution to 49.9°C at the Min. impact solution due to the limited usage heat pump, especially when the damage limits are increased.

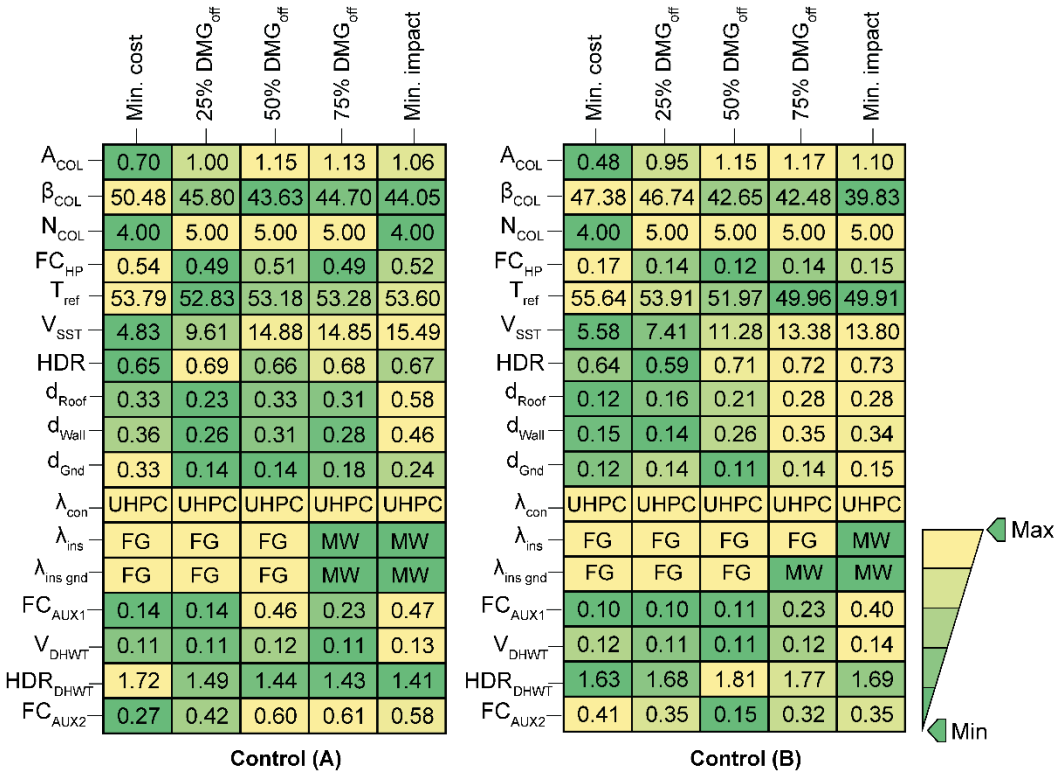

Fig. 8: Pareto optimal solutions of the HP integrated SDHS configuration to cover the demand of 10 buildings located in Madrid under HP control strategy (A) and (B) where the colour map indicates the min and max value of each decision variable.

Comparing the design parameters related to the SST, it is seen that under control (A), the volume of the tank increase from 4.84 to 15.5 $m^3/(MWh \cdot a)$ with the movement toward Min. impact solution. While under control (B), a reduction in the seasonal storage tank volume is indicated by around 2.2 $m^3/(MWh \cdot a)$ for all the optimal configurations except for the Min. cost solution. On the other hand, significant changes are reflected in terms of the thickness of the insulation materials utilized in the SST. When the control (B) is used, the required thickness of the insulation for the roof, walls, and ground is reduced for all the Pareto optimal configurations. In case of the Min. cost solution, a thickness of around 0.3 m is selected for all SST walls under control strategy (A), whereas it is reduced to around 0.13 m under control strategy (B).

Regarding the SST construction, the material that exhibits superior performance in all the scenarios is found to be UHPC. In addition, all the surfaces of the SST select foam glass gravel for the insulation purpose. However, as damage limitations increase, mineral wool is chosen over foam glass, which has a lesser environmental impact. The SST aspect ratio HDR shows limited variations. The auxiliary heater used in the SH distribution circuit is operated less under control (B) which implies less consumption of natural gas. In addition, the DHWT parameters, as well as the auxiliary in the DHW distribution circuit, assume almost constant values under both the proposed control settings.

6.2.1. Cost performance analysis

To perform a comprehensive economic analysis of the proposed SDHS+HP integration, Fig. 9 shows the contributions of investment costs, operational, and replacement costs to the $LCOH$ by different components.

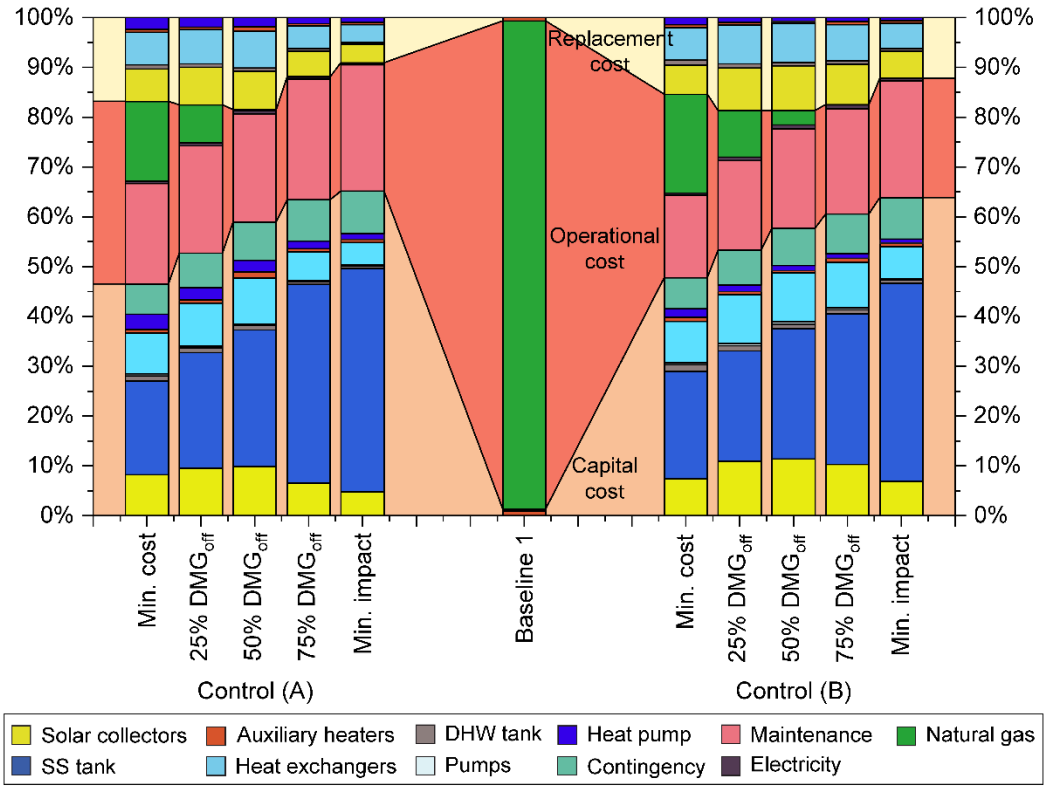

Fig. 9: Breakdown of the $LCOH$ including the shares of initial capital cost, operational cost, and replacement cost for Pareto optimal solutions under HP control strategy (A) and (B) at the five optimal scenarios in comparison to baseline 1. These solutions cover the SH and DHW demands of 10 residential buildings located in Madrid.

By comparing the two-control settings (A) and (B) against the baseline 1 solution, it is observed that the capital cost represents only 1.02% in the baseline 1. While under (A) and (B), the capital cost increases significantly, responsible for up to 65% of the $LCOH$ in case of the Min. impact solution. This high initial investment cost is expected owing to the utilization of solar energy and seasonal thermal energy storage as a heat source in the district heating system. This may be seen as one of the critical barriers to boost the market rollout. The optimal solutions show a noticeable variation from scenario 1 to 5 (from Min. cost to Min. impact), where the SST has the highest share in the $LCOH$, up to 40% in both (A) and (B) control strategies. The capital cost requirements for the SST decreases relatively under the settings (B), which can be attributed to the reduced thickness of the insulation materials used for the SST. Secondly, the investment cost for the heat pump also falls because of the less capacity requirement under (B) where it represents only around 2% compared to 12% in control (A) at the Min. cost solution. The composition of operation cost shows larger shares of natural gas cost under setting (B) compared to (A). This happens since the auxiliary heater is operated more frequently to supply SH with the SST being at a low-temperature level. The replacement cost for the solar collectors shows a similar distribution in the optimization setting (A) and (B). The heat exchangers account for a marginally higher cost of replacement in (B) when the threshold for the environmental damage is increased. In contrast, the replacement cost for the heat pumps is higher in (A) due to its higher capacity.

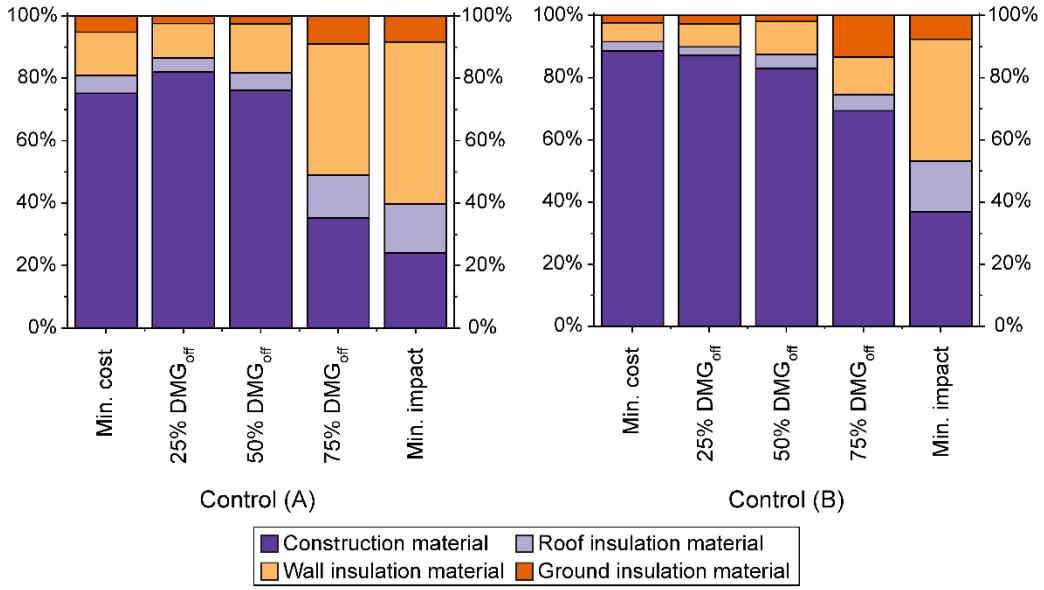

Fig. 10: Cost breakdown for the SST under two different control systems in different damage scenarios.

Since the largest share of capital costs is associated with seasonal storage, it is worth evaluating how the heat pump affects the SST construction and insulation material requirements. As shown in Fig. 10, the majority of the cost is due to the construction material required for the SST. In the case of the minimum cost solution, SDHS with a heat pump featured a higher amount of construction material and less insulation for the roof, wall, and ground when operated under control (B) compared to (A). The values tend to increase moving towards Min. impact solution. This change is expected since the insulation material, which can produce a minimum environmental impact, is relatively expensive. The solutions under control (A) require even more insulation material to minimize the environmental impact.

6.2.2. LCA performance analysis

A detailed analysis of the Pareto fronts in terms of the aggregated ReCiPe 2016 in comparison to the baseline 1 for the different damage scenarios is presented in Fig. 11. In the baseline 1, the consumption of natural gas is responsible for almost 100% of the total impact. For the SDHS +HP configurations, the most significant impact contributors in both (A) and (B) are the solar collectors, natural gas, and seasonal storage tank.

In the case of control strategy (A), the natural gas is responsible for 66.6% and 44.6% share of total environmental impact for scenarios 1 and 2, respectively. When control (B) is applied, the impact of utilizing natural gas as a primary fuel is more prominent since it represents 75.23%, 49.3%, and 21.31% for scenarios 1, 2, and 3, respectively. Moreover, it reduces to a negligible share as we increment the environmental limits (scenarios 4 and 5). Concerning the environmental damage due to the renewable energy technologies used in our SDHS model, the impact of the solar collector increases significantly from 22% in scenario 1 to 70.9% in scenario 5 under the control setting (A). In the case of control (B), it increases from 16.7% to 75.4% (scenarios 1 to 5) as well. It can also be observed that the damage due to the SST shows similar patterns as the collectors. Since the types of construction materials used for the SST were included in the optimization process, its contribution to the total environmental impact has been reduced which is clear from the scenario 4 and 5 in control (A) and scenario 5 in control (B). The impact of the heat pump integrated to SDHS is more prominent under the scheme (A) compared to that of (B) because of its higher fractional capacity. It is evident from Fig. 11 that the consumption of electricity by the heat pump causes negligible environmental damage since the share of impact due to the consumption of electricity

from the grid used to operate the heat pump and the other flow circulation pumps in the SDHS shows the equal distribution in both solutions. This also confirms the importance of the solar collectors, storage tank, and heat pump operating together to reduce the consumption of non-renewable energy sources. This type of analysis could be helpful in determining which carbon tax levels would be needed to push the market towards more renewable technologies.

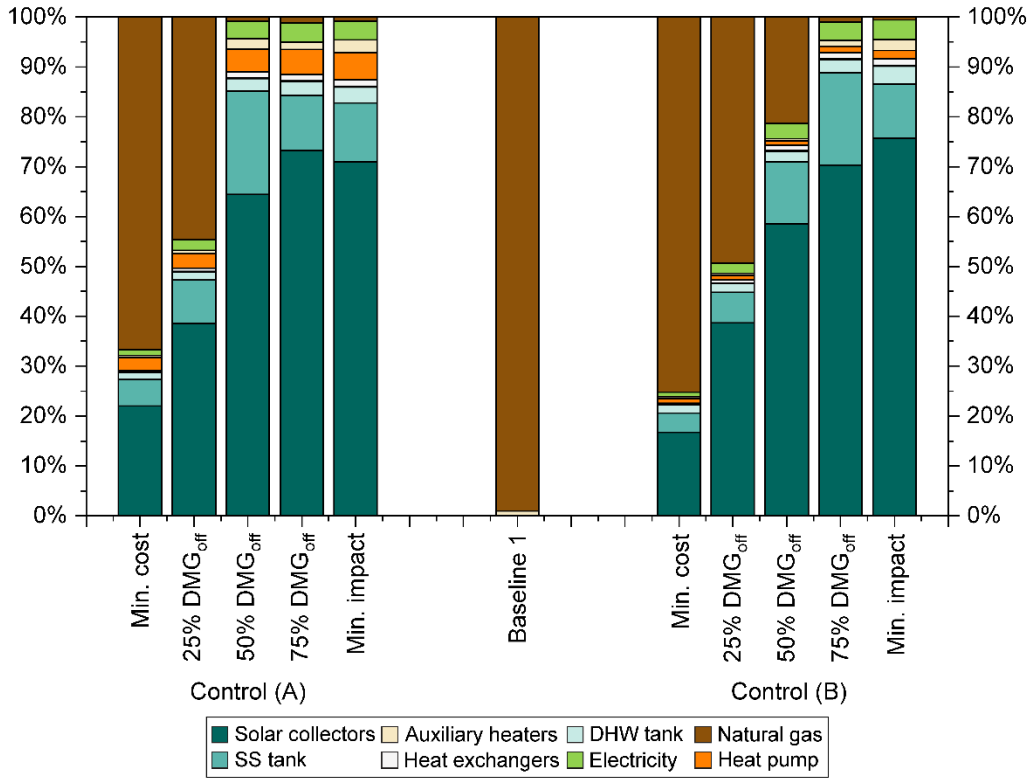

Fig. 11: Breakdown for the aggregated ReCiPe 2016 of Pareto optimal solutions at different damage scenarios for the HP integrated with SDHS applied at control (A) and (B) in comparison to the baseline.

To track the environmental effect of combining heat pump with seasonal storage in a SDHS, Fig. 12 displays the breakdown of the aggregated RCP value for the storage tank under control strategy (A) and (B). The construction of the SST leads to a considerable share of impact; nearly 100% in scenarios 4 and 5 under control (A) and scenario 5 under control (B), which depends on the optimized capacity of the tank. On the other hand, the influence of various insulating materials used in the SST wall, roof, and ground in (A) is 67.4% in scenario 1, 51.9% in scenario 2, and 54.5% in scenario 3. In the case of control (B), the impact due to the insulation slightly reduces to 43% in scenario 1, 44.2% in scenario 2, and 48.2% in scenario 3. The optimization methodology selects the minimum value of the insulation material with minimum impact when we move towards the minimum impact solution. Therefore, in scenarios 4 and 5 under control (A) and scenario 5 under control (B), virtually zero environmental effects are caused by SST insulation. Consequently, the control scheme (B) appears to be marginally advantageous in terms of produced environmental impacts.

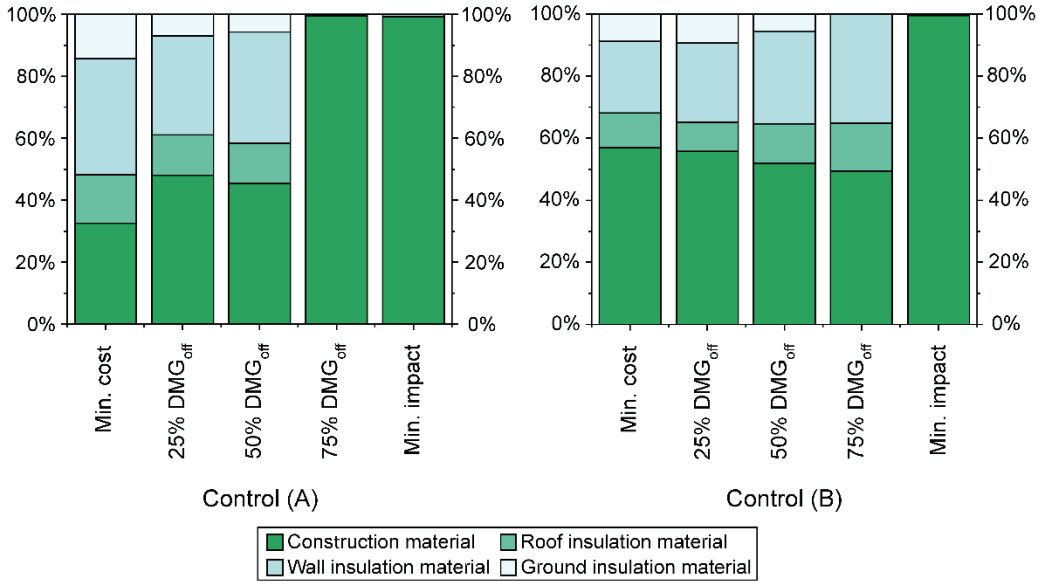

Fig. 12: Breakdown for the aggregated ReCiPe 2016 for the SST at different control strategies under different damage scenarios.

6.2.3. Energy performance analysis

Fig. 13 presents the values of the energy performance indicators achieved by the combination of SDSH and HP with control strategy (A) and (B). As seen from the figure, both (A) and (B) provided almost similar results for η_{COL} with the change in scenarios except for the minimum cost solution. This shows a pleasant correspondence with the previously mentioned values of the solar collector area and the highest value of η_{COL}(72%) obtained in the scenario 1 under control (B) when the size of the collector field assumes the smallest value.

The efficiency of the DHWT η_{DHWT} is very high (around 97%) for all scenarios since it is used as diurnal storage in the district heating network with a limited heat loss to the environment. Regarding the performance of the space heating circuit, under control (A), values of η_{SST} remain almost alike following the heat loss from the SST throughout the environmental damage scenarios, as seen in Fig. 13. On the other hand, the overall heat loss coefficient of the SST in control (A) initially increases and then decreases. At the same time, in control (B), it diminishes consistently with increasing the limit of damage to the environment. This is due to the optimized geometry and materials used for the construction and insulation of the SST. The highest efficiency obtained for the SST is 92% for the Min. impact solution under control (A), which also has the minimum value of heat loss coefficient (0.075W/m^2). The efficiency of the storage is compromised under control (B) since this control setting uses the heat pump to stabilize the storage temperature reducing the use of insulation material for the SST, which in turn increases the heat loss. In terms of the solar fraction, it is improved from 79% in control (A) to 86% in control (B) under Min. cost-optimal scenario. For the rest of the scenarios, the SF_{global} rises progressively with the increment in the environmental damage limits approaching almost 100% for the minimum impact solution. This can be explained with the expanded installation of renewable energy equipment in the district heating sector. The seasonal performance factor of the heat pump shows improvement under (B) compared to (A) when we look into the scenarios 1 to 3. The highest value of SPF_{HP} is 6.01 for the minimum cost solution in (B). However, when the methodology aims for the minimum environmental impact, the efficiency of the heat pump is compromised.

The next step in this analysis is the evaluation of the proposed design of SDHS operating under the superior control system (B) in comparison to a previously examined SDHS configuration without heat pump (Baseline 2) as presented by Abokersh et al. [42].

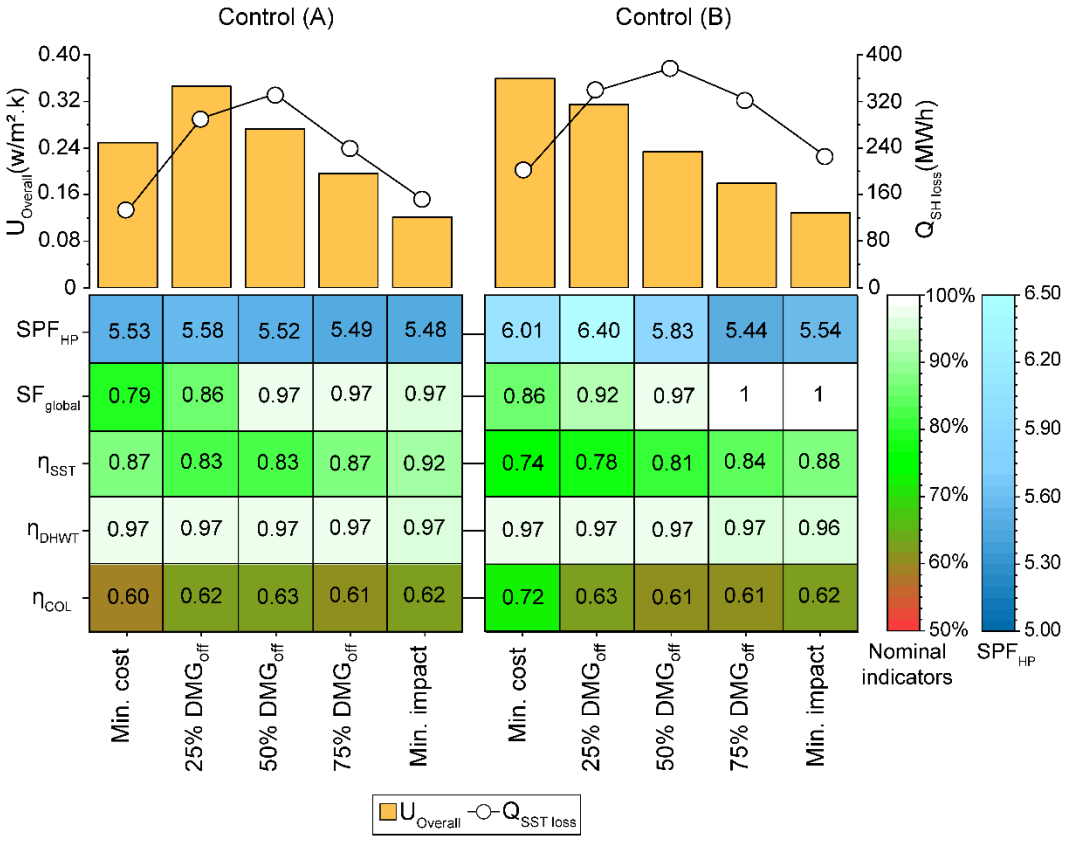

Fig. 13: Thermal performance indicators for the optimal Pareto solutions of SDHS under HP control strategy (A) and (B). These designs satisfy the SH and DHW demand of the 10 residential buildings located in Madrid.

6.3. The effect of integrating HP into SDHS

The Pareto optimal solutions under control (B) are compared with the results from Abokersh et al. [42](baseline 2) to establish the value addition made by the integration of the heat pump to SDHS while covering the SH and DHW demand of 10 residential buildings located in Madrid to achieve the 4GDH goals. It was observed in Fig. 14(a) that coupling of a heat pump in between the solar collector and the seasonal storage tank could result in better cost-effectiveness for the SDHS network. The new configuration reduced the $LCOH$ from 62.5 €/MWh to 59.1 €/MWh (5.44%) in the case of the Min. cost solution. This is followed by the rest of the Pareto optimal solutions, which are also marginally cost-beneficial. Besides, the payback period of the new system configuration is significantly reduced under all damage scenarios. The Min. cost-optimal solution with the heat pump added to the SDHS has the lowest value of the payback period, i.e., 26 years in comparison to the baseline 2 scenario. However, this still very high payback period is due to two main reasons; firstly, the low natural gas prices [72] which keep the operational cost of the natural gas boiler a competitive solution with the SDHS. Secondly, all the optimal solutions of the SDHS have a high solar fraction above 85%, which is the cause of a high investment cost due to the extensive usage for renewable energy components. Since the system lifetime is assumed to be 40 years, the Min. cost solution seems reasonable to adapt to implement the proposed SDHS with the control system (B) as a 4GDH system.

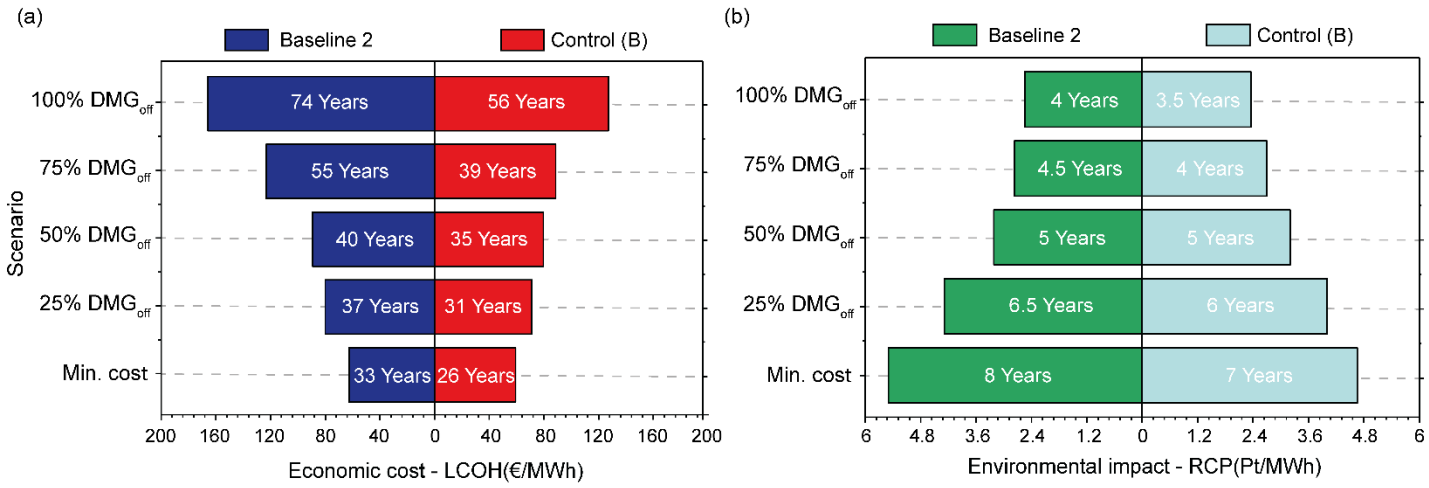

Fig. 14: Various Pareto optimal solutions comprising of the objective functions for the HP integrated with SDHS under control strategies (B) in comparison to the baseline 2in terms of (a) the $LCOH$ and PB objectives, and (b) theRCP and $GPBP$ objectives.

Regarding environmental sustainability, the values of environmental damage indicator RCP and $GPBP$for the HP integrated with SDHS are reasonably comparable with baseline 2, as shown in Fig. 14(b). The optimal solution for minimum cost with a heat pump has an impact of 4.65 Pt/MWh with the largest $GPBP$ (7 years) against the baseline 2 with an impact of 5.49 Pt/MWh and $GPBP$ of 8 years. The environmental impact of both configurations reduces if moved towards the 100% damage limit. Hence, it can be concluded that the addition of the heat pump makes the SDHS more sustainable, although the heat pump runs on the electricity from the grid.

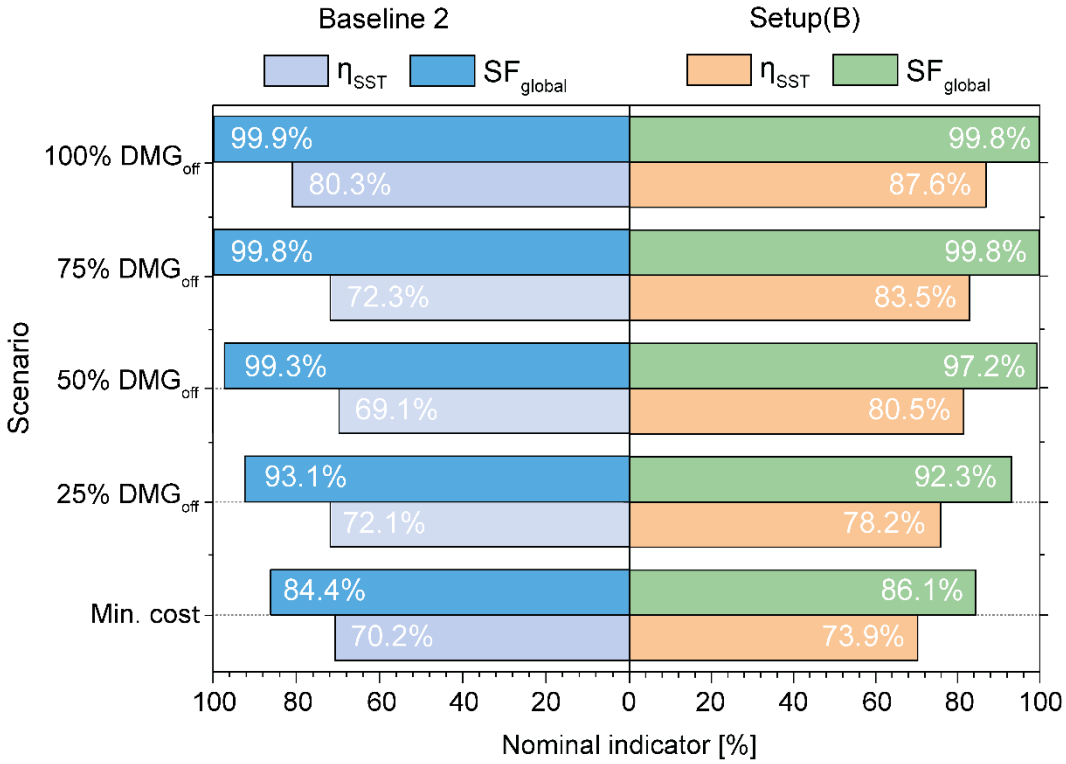

Fig. 15: Thermal performance indicators for the optimal Pareto solutions for HP integrated with SDHS under control strategy (B) in comparison to baseline 2.

Based on the comparison presented in Fig. 15, one can observe that the thermal efficiency of the seasonal storage tank in SDHS +HP is higher than that of baseline 2. The heat pump enhances the value of η_{SST} by 5% in damage scenario 1, 7.8% in scenario 2, 14.2% in scenario 3, 13.4% in scenario 4, and 8.3% in scenario 5 compared to baseline 2. Regarding the overall solar fraction of the system, only the Min. cost solution with an integrated heat pump shows a slightly higher value of SF_{global}(86.1%) than the baseline 2 (84.4%). All other optimal solutions (scenarios 2 to 5) have marginally less value of SF_{global} and remain energetically competitive with the baseline 2 configuration. Therefore, if the Min. cost solution of the SDHS has to be chosen to establish the economic feasibility of a 4GDH network, the incorporation of the heat pump into the SDHS and seasonal storage with optimal control (B) proves to be a better decision in terms of energy efficiency as well.

The above analysis of the comparison between the HP integrated SDHS under control strategy (B), and the baseline 2 (without heat pump) shows again that the minimum cost solution is a favorable choice considering economic, environmental and energy performance. Hence, finally, we compare these two configurations using the optimized values of the decision variables in both cases, as shown in Table 3. In the heat supply circuit, by adding the heat pump, a reduction of 12.9% in the collector area is achieved compared to the baseline 2. This indicates that the heat pump is able to bring down the SDHS temperature levels to operate as a 4GDH and subsequently reduces the requirement to add more insulation materials, as shown in Fig. 16.

Concerning the SH circuit, the volume of seasonal storage is increased from 4.96 m^3/(MWh·a) to 5.58 m^3/(MWh·a) (11.1%). However, the requirement of insulation materials is reduced significantly for the roof by 76.9%, 50% for the sidewalls, and 71.4% for the bottom of the SST due to the rule of the heat pump in reducing the SST temperature level. This reduction is reflected in the investment cost. This is followed by the change in the SST aspect ratio from 0.68 to 0.64. The optimization methodology selects the same type of materials for the construction and insulation of the SST. The heat pump did not have an impact on the size of the auxiliary heater required in the SH circuit as a backup. To supply the DHW demand using the HP+SDHS, the auxiliary heater is used more often than the baseline 2. This leads to an increase in terms of its fractional capacity (0.34 to 0.41) due to the limited capacity of the HP. The required volume of the DHWT remains the same, although the aspect ratio of the tank has differed.

The investment cost is reduced to 2.15 million Euros from 2.24 million Euros for the SHDH system equipped with the heat pump in the presented optimization results. The additional investment cost due to the heat pump does not affect the SDHS configuration. Instead, it helps to improve the overall system efficiency by lowering the capital investment on the solar collectors and the seasonal storage by 4% as compared to baseline 2. Furthermore, the operation cost is also decreased in the current study by 11.2% because of the lower operating temperatures yield. However, the replacement cost increases due to the use of the heat pump over the system lifetime.

Table 3: The Pareto minimum cost-optimal configuration and its relative cost breakdown for the HP integrated SDHS under control strategy (B) in comparison to baseline 2.

	Circuit Name	Parameter	Unit	Baseline 2	Control (B)
Decision variables	Supply Circuit	Heat demand	(MWh·a)	1913.4	1913.4
		A_{COL}	m^2/(MWh·a)	0.54	0.47
		β_{COL}	º	45.4	47.3
		N_{COL}	-	4	4
		FC_{HP}	-	-	0.17

	SH circuit	V_{SST}	$m^3/(MWh \cdot a)$	4.96	5.58
		HDR	m/m	0.68	0.64
		d_{Roof}	m	0.52	0.12
		d_{Wall}	m	0.30	0.15
		d_{Gnd}	m	0.42	0.12
		λ_{con}	W/(m·K)	UHPC	UHPC
		λ_{ins}	W/(m·K)	FG	FG
		$\lambda_{ins\ gnd}$	W/(m·K)	FG	FG
		FC_{AUX1}	-	0.10	0.10
	DHW Circuit	V_{DWHT}	$m^3/(MWh \cdot a)$	0.12	0.12
		HDR_{DHWT}	m/m	1.80	1.63
		FC_{AUX2}	-	0.34	0.41
$LCOH$ parameters	Investment cost	C_C	Million Euros	2.24	2.15
	Operational cost	C_O	Million Euros	1.87	1.66
	Replacement cost	C_R	Million Euros	0.67	0.69

Additionally, Fig. 16 shows the differences in temperature profiles within the solar thermal collectors and the seasonal storage tank over a year. Adding the heat pump under control strategy (B) has helped to keep the temperature low for the collector, especially during September, and it never exceeds 80°C. In contrast, it goes up to 104.5°C at baseline 2. Furthermore, the temperature inside the storage is also reduced to 85.4°C in October compared to 87.6°C in baseline 2. This lowers the temperature difference between the heat source (collector) and the heat sink (storage) for the heat pump resulting in a higher value of SST efficiency as well as a higher HP seasonal performance factor.

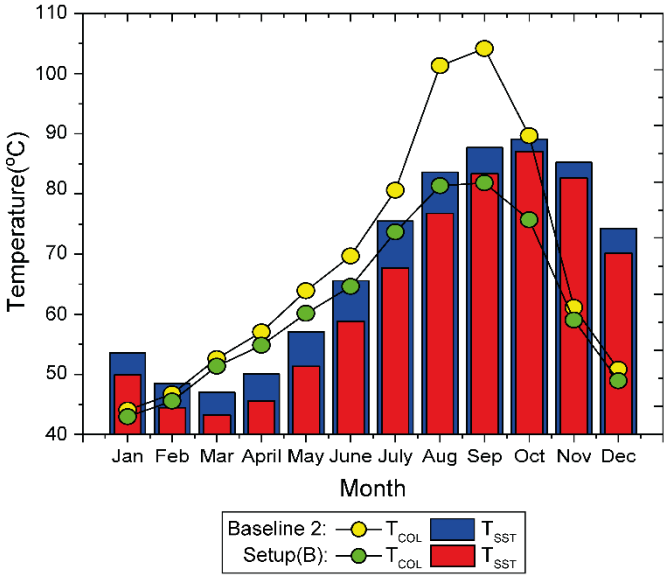

Fig. 16: The monthly temperature profiles of the solar collector field and SST for the HP integrated with SDHS under control strategy (B) in comparison to baseline 2 for the minimum cost-optimal solution.

6.4. The impact of heat pump and seasonal storage in SDHS for reaching 4GDH targets

This section aims to answer the research question about whether the proposed configuration of SDHS enhanced with seasonal storage and heat pump for a district heating scenario can fulfill the target

characteristics of a 4GDH system. The selected KPIs are based on the perspectives of three key stakeholders of district heating, as explained in section 3.4 and derived as a percentage of the target value of a 4GDH system for the minimum cost configuration of the SDHS among all the Pareto optimal points.

It is evident from Fig. 17 that the energy KPIs have the potential to reach the 4GDH goals. Due to the implementation of the solar thermal collector with seasonal storage and heat pump technology using an optimal control strategy (B), the share of renewable energy, i.e. the solar fraction has been able to reach 86.1% of the total heating demand. This minimizes the use of fossil fuel for district heating and thus promotes a transition towards a low-carbon system. The coupling of the heat pump in order to directly supply the storage has resulted in a very high value of SPF_{HP} (6.01), although it is operated for small durations. This complies with the KPI target value by 100%. The temperature barrier for low-temperature district heating appears to be removed since the supply and return temperature in the proposed SDHS is maintained at 50/30°C. This is in line with the target temperature range of the 4GDH network by 80%, which is a major feature to be present in a 4GDH system. Concerning the seasonal storage integration into 4GDH, the temperature inside the storage tank is at 93.2% of the desired value. Nevertheless, the proposed model has been entirely successful in keeping the collector temperature low. The efficiency of the storage is found less than the expected level due to the heat losses to the ambient. Overall, the technical suitability of the SDHS model is established to transform into a 4GDH system.

The financial KPIs in our study ($LCOH$) have shown that the cost at which the system must supply heat to the customers at 50°C is reduced by 34.2% compared to the local heat price for the natural gas-based district heating system. The reduction in the payback period is estimated to be about 35% as well. Hence, the SDHS carries potential economic benefits over the traditional district heat supply to be operated as a 4GDH for each potential district heating investor. This also highlights that the usage of low-temperature heat sources does not have financial disadvantages for the potential expansion of district heating networks into 4GDH. However, it calls for long-term financial commitments to become competitive.

When it comes to environmental impact and the policy decision-makers, the corresponding KPIs (RCP and $GPBP$) reflect that SDHS can be successful in reducing the adverse environmental effects of the natural gas-based conventional system by 82.5% while delivering energy for 40 years of operational lifetime. Therefore, the proposed configuration of SDHS can help to transform into a future 4GDH producing a minimum carbon footprint. It also highlights the importance to orchestrate policies for deploying technologies as renewable as possible for building district heating systems in the future.

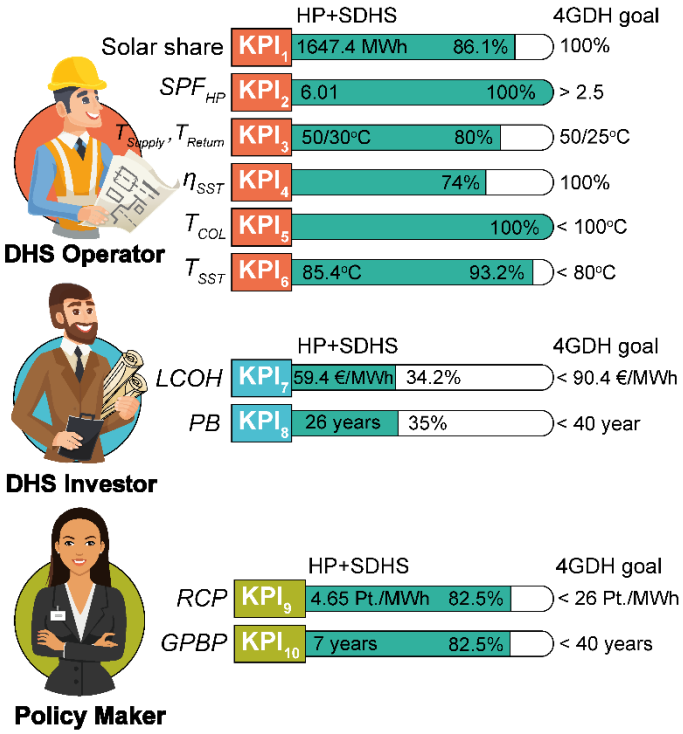

Fig. 17: KPI achievement rates for the HP integrated with SDHS under control strategy (B) as a part of the 4GDH target.

The overall discussion with KPIs thus indicates that the SDHS model presented in this study can successfully integrate low- temperature renewable heat source, i.e., solar thermal with seasonal and short-term storages with the help of an intelligently controlled heat pump. These technical improvements result in significant economic and sustainability motivations for the concerning stakeholders as compared to the traditional heat supply structures. Therefore, this configuration can be implemented as a 4GDH system in the future district energy systems.

With respect to potential district heating systems stakeholders, the KPIs mentioned above will allow them to have a better understanding of the business assets and to make informed decisions. For every KPI, however, not all the stakeholders have the same priority. DH companies interested in improving the thermal network would be more concerned about the energy and economic KPIs of 4GDH. The importance of environmentally friendly DH technologies typically goes unattended by both network operators and consumers at present. The environmental KPIs, however, provide the policymakers with valuable insight to encourage large-scale DH infrastructures. Furthermore, there may be incoherence between state and local governments with respect to energy policies. For this reason, it is expected that the introduction of sustainable technical solutions such as SDHS and transition towards the 4GDH would yield better results when local legislative authorities and DH operators/owners work together.

7. Conclusion

This paper tends to optimize the performance of a heat pump (HP) enhanced solar assisted district heating system (SDHS) with seasonal storage to facilitate space heating (SH) and domestic hot water (DHW)for a hypothetical urban community located in Madrid, Spain. A multi-objective optimization methodology based on an artificial neural network (ANN) model is adopted through TRNSYS simulations. The objectives that

are minimized in this study are cost and aggregated environmental impact while maximizing the energy efficiency of the SDHS model. Two different control strategies are applied to investigate the scope of improving the system stability and overall performance of the network to promote SDHS for implementation as a 4th generation district heating (4GDH). To compare the performance of the proposed system, two baseline scenarios are presented; the conventional heating systems based on natural gas and an optimized SDHS model without integrating the heat pump. The following is a summary of our study's principal findings:

- The ANN model prediction is found to be highly accurate and hence used in our study to train and predict the performance of the SDHS model.
- Compared to the traditional district heating system fuelled with natural gas, the estimated Min. cost-optimal solution for the configuration SDHS + HP achieves significant economic and environmental benefits. Under the control system (A), the life cycle cost is reduced to 72.1 €/MWh from 90.3 €/MWh while the environmental impact reduces by 80.6%. These values reduce further to 59.1 €/MWh and 82.5% when the control system (B) is applied. Also, control (B) has been able to outperform control (A) in reducing the consumption of grid electricity by the SDHS by 90%.
- Similar to the economic and environmental results, the energy efficiency of the solar thermal collectors and the solar fraction of the proposed configuration is higher when SDHS is operated under control setting (B) as well as the heat pump has a better seasonal performance factor. The efficiency of seasonal storage is decreased by 17.5% due to the increased amount of heat loss from the storage tank in comparison to control (A). Furthermore, the annual thermal energy profiles of the Min. cost Pareto optimized solutions show that the optimal control strategy (B) can build a better balance between the different heat sources, i.e., the solar collector, storage tanks, heat pump and auxiliary heaters leading to stable performance of the system. This highlights the effectiveness of control (B) to properly integrate a heat pump and seasonal thermal energy storage into a SDHS so that overall efficiency is improved.
- The techno-economic advantages of adding a heat pump into the SDHS with the aid of control strategy (B) is established further by comparing its performance with the second baseline system (SDHS without HP). The SDHS+HP configuration remarkably reduces the solar collector area and the SST insulation requirement, which causes the initial investment and operating cost to be reduced. This allows a return on the investment within the first 26 years of the project lifetime. The new configuration also lowers the temperature level of the collector and the SST, thereby raising the SH efficiency and total solar fraction. Considering the environmental impact, the SDHS+HP produces slightly lesser ecological damage. Thus, investing in a heat pump seems to be a smart policy. The cost associated with the heat pump is compensated by improved energy, economic and sustainable performance of the SDHS.
- The optimization methodology has resulted in several KPI scores for the SDHS, which are consistent with the target KPIs of the 4GDH concept. The combination of the solar thermal with seasonal storage for space heating along with a heat pump to stabilize the overall system performance is close enough to a 4GDH. The supply and return temperature of the SDHS is maintained at 50/30°C while covering 86.1%of the heat demand using renewable energy. Finally, it shows that even if the initial cost of introducing a SDHS+HP system may look like a financial bottleneck for investors, in the long run, this new configuration has huge potential to generate revenue and as well as helping in decarbonizing the DH sector.

In conclusion, the presented research work shows SDHS assisted with HP can be an attractive energy solution that can lead to substantial techno-economic and environmental benefits over conventional heating systems if the influential design parameters are optimized using a smart control strategy. Furthermore, our study highlights the suitability of the combined configuration of solar thermal energy, seasonal storage, and heat pump as a 4GDH system. The results of this multi-perspective analysis can be used by the key

stakeholders as a starting point to develop necessary business models. Future research should concentrate on optimizing the architecture of the thermal distribution grid and improving energy efficiency at the end-user. This will allow the full competitiveness of SDHS for the sustainable energy transition.

Acknowledgements

The work is funded by the Spanish government RTI2018-093849-B-C31 and RTI2018-093849-B-C33. The authors would like to thank the Catalan Government for the quality accreditation given to their research group (GREiA - 2017 SGR 1537, AGACAPE - 2017 SGR 1409). GREiA is a certified agent TECNIO in the category of technology developers from the Government of Catalonia. This work is partially supported by ICREA under the ICREA Academia programme. This work is partially funded by the Ministerio de Ciencia, Innovación y Universidades – Agencia Estatal de Investigación (AEI) (RED2018-102431-T). This project has received funding from the European Union's Horizon 2020 research and innovation programme under the Marie Skłodowska-Curie grant agreement No. 713679 and from the Universitat Rovira i Virgili (URV).

References

[1] EAA. Trends and projections in Europe 2019. 2019. doi:10.2800/51114.

[2] Lund H, Østergaard PA, Connolly D, Mathiesen BV. Smart energy and smart energy systems. Energy 2017. doi:10.1016/j.energy.2017.05.123.

[3] Lund H, Duic N, Østergaard PA, Mathiesen BV. Smart energy systems and 4th generation district heating. Energy 2016. doi:10.1016/j.energy.2016.07.105.

[4] Connolly D, Lund H, Mathiesen B V., Werner S, Möller B, Persson U, et al. Heat roadmap Europe: Combining district heating with heat savings to decarbonise the EU energy system. Energy Policy 2014. doi:10.1016/j.enpol.2013.10.035.

[5] Lund H, Duic N, Østergaard PA, Mathiesen BV. Future district heating systems and technologies: On the role of smart energy systems and 4th generation district heating. Energy 2018. doi:10.1016/j.energy.2018.09.115.

[6] Schmidt D, Kallert A, Blesl M, Svendsen S, Li H, Nord N, et al. Low Temperature District Heating for Future Energy Systems. Energy Procedia, 2017. doi:10.1016/j.egypro.2017.05.052.

[7] Buffa S, Cozzini M, D'Antoni M, Baratieri M, Fedrizzi R. 5th generation district heating and cooling systems: A review of existing cases in Europe. Renew Sustain Energy Rev 2019. doi:10.1016/j.rser.2018.12.059.

[8] Prando D, Prada A, Ochs F, Gasparella A, Baratieri M. Analysis of the energy and economic impact of cost-optimal buildings refurbishment on district heating systems. Sci Technol Built Environ 2015. doi:10.1080/23744731.2015.1040343.

[9] Li H, Nord N. Transition to the 4th generation district heating - Possibilities, bottlenecks, and challenges. Energy Procedia, 2018. doi:10.1016/j.egypro.2018.08.213.

[10] Lygnerud K. Business model changes in district heating: The impact of the technology shift from the third to the fourth generation. Energies 2019. doi:10.3390/en12091778.

[11] Guzzini A, Pellegrini M, Pelliconi E, Saccani C. Low temperature district heating: An expert opinion survey. Energies 2020. doi:10.3390/en13040810.

[12] Hmadi M, Mourtada A, Daou R. Forecasting the performance of a district solar thermal smart network in desert climate – A case study. Energy Convers Manag 2020;207:112521. doi:10.1016/j.enconman.2020.112521.

[13] Provasnek AK, Putz S. IEA SHC task 55: Towards the integration of large SHC systems into DHC networks. ISES Sol. World Congr. 2017 - IEA SHC Int. Conf. Sol. Heat. Cool. Build. Ind. 2017, Proc., 2017. doi:10.18086/swc.2017.06.10.

[14] Weiss W, Spörk-Dür M. Solar Heat Worldwide 2018. Global Market Development and Trends in 2017. Detailed Market Figures 2016. IEA Sol Heat Cool Program 2018. doi:10.1017/CBO9781107415324.004.

[15] Xu L, Torrens JI, Guo F, Yang X, Hensen JLM. Application of large underground seasonal thermal energy storage in district heating system: A model-based energy performance assessment of a pilot system in Chifeng, China. Appl Therm Eng 2018. doi:10.1016/j.applthermaleng.2018.03.047.

[16] Dahash A, Ochs F, Janetti MB, Streicher W. Advances in seasonal thermal energy storage for solar

district heating applications: A critical review on large-scale hot-water tank and pit thermal energy storage systems. Appl Energy 2019;239:296–315. doi:10.1016/j.apenergy.2019.01.189.

[17] Hesaraki A, Holmberg S, Haghighat F. Seasonal thermal energy storage with heat pumps and low temperatures in building projects - A comparative review. Renew Sustain Energy Rev 2015;43:1199–213. doi:10.1016/j.rser.2014.12.002.

[18] Chwieduk DA. Solar-assisted heat pumps. Compr. Renew. Energy, 2012. doi:10.1016/B978-0-08-087872-0.00321-8.

[19] Marx R, Bauer D, Drueck H. Energy Efficient Integration of Heat Pumps into Solar District Heating Systems with Seasonal Thermal Energy Storage. Energy Procedia, 2014. doi:10.1016/j.egypro.2014.10.302.

[20] David A, Mathiesen BV, Averfalk H, Werner S, Lund H. Heat Roadmap Europe: Large-scale electric heat pumps in district heating systems. Energies 2017. doi:10.3390/en10040578.

[21] Tschopp D, Tian Z, Berberich M, Fan J, Perers B, Furbo S. Large-scale solar thermal systems in leading countries: A review and comparative study of Denmark, China, Germany and Austria. Appl Energy 2020;270:114997. doi:10.1016/j.apenergy.2020.114997.

[22] Garcia NP, Vatopoulos K, Lopez AP, Thiel C. Best available technologies for the heat and cooling market in the European Union. JRC Scientif and Policy Reports. 2012. doi:10.2790/5813.

[23] Song Z, Ji J, Cai J, Li Z, Gao Y. Performance prediction on a novel solar assisted heat pump with hybrid Fresnel PV plus TEG evaporator. Energy Convers Manag 2020;210:112651. doi:10.1016/j.enconman.2020.112651.

[24] Pardo García N, Zubi G, Pasaoglu G, Dufo-López R. Photovoltaic thermal hybrid solar collector and district heating configurations for a Central European multi-family house. Energy Convers Manag 2017;148:915–24. doi:10.1016/j.enconman.2017.05.065.

[25] Chaturvedi SK, Gagrani VD, Abdel-Salam TM. Solar-assisted heat pump - A sustainable system for low-temperature water heating applications. Energy Convers Manag 2014. doi:10.1016/j.enconman.2013.09.050.

[26] Sterling SJ, Collins MR. Feasibility analysis of an indirect heat pump assisted solar domestic hot water system. Appl Energy 2012. doi:10.1016/j.apenergy.2011.05.050.

[27] Kim T, Choi B Il, Han YS, Do KH. A comparative investigation of solar-assisted heat pumps with solar thermal collectors for a hot water supply system. Energy Convers Manag 2018. doi:10.1016/j.enconman.2018.07.035.

[28] Banister CJ, Collins MR. Development and performance of a dual tank solar-assisted heat pump system. Appl Energy 2015. doi:10.1016/j.apenergy.2015.03.130.

[29] Kim MH, Kim D, Heo J, Lee DW. Techno-economic analysis of hybrid renewable energy system with solar district heating for net zero energy community. Energy 2019. doi:10.1016/j.energy.2019.115916.

[30] Østergaard PA, Andersen AN. Economic feasibility of booster heat pumps in heat pump-based district heating systems. Energy 2018. doi:10.1016/j.energy.2018.05.076.

[31] Hirvonen J, ur Rehman H, Sirén K. Techno-economic optimization and analysis of a high latitude solar district heating system with seasonal storage, considering different community sizes. Sol

Energy 2018;162:472–88. doi:10.1016/j.solener.2018.01.052.

[32] Rehman H ur, Hirvonen J, Sirén K. Performance comparison between optimized design of a centralized and semi-decentralized community size solar district heating system. Appl Energy 2018;229:1072–94. doi:10.1016/j.apenergy.2018.08.064.

[33] Khorasaninejad E, Hajabdollahi H. Thermo-economic and environmental optimization of solar assisted heat pump by using multi-objective particle swam algorithm. Energy 2014;72:680–90. doi:10.1016/j.energy.2014.05.095.

[34] Fazlollahi S, Becker G, Ashouri A, Maréchal F. Multi-objective, multi-period optimization of district energy systems: IV - A case study. Energy 2015;84:365–81. doi:10.1016/j.energy.2015.03.003.

[35] Kalogirou SA. Applications of artificial neural-networks for energy systems. Appl Energy 2000. doi:10.1016/S0306-2619(00)00005-2.

[36] Kumar R, Aggarwal RK, Sharma JD. Energy analysis of a building using artificial neural network: A review. Energy Build 2013. doi:10.1016/j.enbuild.2013.06.007.

[37] Wong SL, Wan KKW, Lam TNT. Artificial neural networks for energy analysis of office buildings with daylighting. Appl Energy 2010;87:551–7. doi:10.1016/j.apenergy.2009.06.028.

[38] Esen H, Inalli M, Sengur A, Esen M. Performance prediction of a ground-coupled heat pump system using artificial neural networks. Expert Syst Appl 2008. doi:10.1016/j.eswa.2007.08.081.

[39] Xia L, Ma Z, Kokogiannakis G, Wang Z, Wang S. A model-based design optimization strategy for ground source heat pump systems with integrated photovoltaic thermal collectors. Appl Energy 2018;214:178–90. doi:10.1016/j.apenergy.2018.01.067.

[40] Hirvonen J, ur Rehman H, Deb K, Sirén K. Neural network metamodelling in multi-objective optimization of a high latitude solar community. Sol Energy 2017. doi:10.1016/j.solener.2017.06.040.

[41] Tulus V, Abokersh MH, Cabeza LF, Vallès M, Jiménez L, Boer D. Economic and environmental potential for solar assisted central heating plants in the EU residential sector: Contribution to the 2030 climate and energy EU agenda. Appl Energy 2019. doi:10.1016/j.apenergy.2018.11.094.

[42] Abokersh MH, Vallès M, Cabeza LF, Boer D. A framework for the optimal integration of solar assisted district heating in different urban sized communities : A robust machine learning approach incorporating global sensitivity analysis. Appl Energy 2020;267:114903. doi:10.1016/j.apenergy.2020.114903.

[43] Rehman H ur, Hirvonen J, Sirén K. Influence of technical failures on the performance of an optimized community-size solar heating system in Nordic conditions. J Clean Prod 2018;175:624–40. doi:10.1016/j.jclepro.2017.12.088.

[44] United Nations Environment Programme, Solar Thermal Energy Technology Fact Sheet. 2014.

[45] Hobbi A, Siddiqui K. Optimal design of a forced circulation solar water heating system for a residential unit in cold climate using TRNSYS. Sol Energy 2009;83:700–14. doi:10.1016/j.solener.2008.10.018.

[46] Hui L, Edem NTK, Nolwenn LP, Lingai L. Evaluation of a seasonal storage system of solar energy for house heating using different absorption couples. Energy Convers Manag 2011;52:2427–36. doi:10.1016/j.enconman.2010.12.049.

[47] Lorenzo C, Narvarte L. Performance indicators of photovoltaic heat-pumps. Heliyon 2019;5:e02691. doi:10.1016/j.heliyon.2019.e02691.

[48] Hang Y, Qu M, Ukkusuri S. Optimizing the design of a solar cooling system using central composite design techniques. Energy Build 2011;43:988–94. doi:10.1016/j.enbuild.2010.12.024.

[49] Allouhi A, Agrouaz Y, Benzakour Amine M, Rehman S, Buker MS, Kousksou T, et al. Design optimization of a multi-temperature solar thermal heating system for an industrial process. Appl Energy 2017;206:382–92. doi:10.1016/j.apenergy.2017.08.196.

[50] Welsch B, Göllner-Völker L, Schulte DO, Bär K, Sass I, Schebek L. Environmental and economic assessment of borehole thermal energy storage in district heating systems. Appl Energy 2018;216:73–90. doi:10.1016/j.apenergy.2018.02.011.

[51] Gabbrielli R, Castrataro P, Del Medico F, Di Palo M, Lenzo B. Levelized cost of heat for linear Fresnel concentrated solar systems. Energy Procedia, 2014. doi:10.1016/j.egypro.2014.03.143.

[52] Kalogirou SA. Solar Energy Engineering: Processes and Systems. Second edi. Amsterdam: Elsevier Inc.; 2014. doi:10.1007/978-3-662-49120-1_32.

[53] Buonomano A, Calise F, Palombo A, Vicidomini M. Transient analysis , exergy and thermo-economic modelling of façade integrated photovoltaic / thermal solar collectors. Renew Energy 2019;137:109–26. doi:10.1016/j.renene.2017.11.060.

[54] Guillén-Gosálbez G, Caballero JA, Jiménez L. Application of Life Cycle Assessment to the Structural Optimization of Process Flowsheets. Ind Eng Chem Res 2008;47:777–89. doi:10.1016/S1570-7946(07)80218-5.

[55] Goedkoop M, Heijungs R, Huijbregts M, Schryver A De, Struijs J, Zelm R Van. ReCiPe 2008, A life cycle impact assessment method which comprises harmonised category indicators at the midpoint and the endpoint level. First edition. Report I: Characterisation. 2009.

[56] Gursel AP, Ostertag C. Comparative life-cycle impact assessment of concrete manufacturing in Singapore. Int J Life Cycle Assess 2017. doi:10.1007/s11367-016-1149-y.

[57] Li DHW, Lam TNT, Chan WWH, Mak AHL. Energy and cost analysis of semi-transparent photovoltaic in office buildings. Appl Energy 2009;86:722–9. doi:10.1016/j.apenergy.2008.08.009.

[58] Dammeier LC, Loriaux JM, Steinmann ZJN, Smits DA, Wijnant IL, Van Den Hurk B, et al. Space, Time, and Size Dependencies of Greenhouse Gas Payback Times of Wind Turbines in Northwestern Europe. Environ Sci Technol 2019;53:9289–97. doi:10.1021/acs.est.9b01030.

[59] Gibb D, Johnson M, Romaní J, Gasia J, Cabeza LF, Seitz A. Process integration of thermal energy storage systems – Evaluation methodology and case studies. Appl Energy 2018;230:750–60. doi:10.1016/j.apenergy.2018.09.001.

[60] Volkova A, Ma V, Siirde A. Methodology for evaluating the transition process dynamics towards 4th generation district heating networks 2018;150. doi:10.1016/j.energy.2018.02.123.

[61] Kucherenko S, Albrecht D, Saltelli A. Exploring multi-dimensional spaces: a Comparison of Latin Hypercube and Quasi Monte Carlo Sampling Techniques. 8th IMACS Semin. Monte Carlo methods, 2015, p. 1–32. doi:10.1016/j.ress.2017. 04.003.

[62] Bauer D, Marx R, Nußbicker-Lux J, Ochs F, Heidemann W, Müller-Steinhagen H. German central solar heating plants with seasonal heat storage. Sol Energy 2010;84:612–23.

doi:10.1016/j.solener.2009.05.013.

[63] Solites. Guideline for Seasonal Thermal Energy Storage Systems in the Built Environment. Stuttgart: 2016.

[64] Konak A, Coit DW, Smith AE. Multi-objective optimization using genetic algorithms : A tutorial. Reliab Eng Syst Saf 2006;91:992–1007. doi:10.1016/j.ress.2005.11.018.

[65] Ibrahim D, Jobson M, Li J, Guillén-Gosálbez G. Optimization-based design of crude oil distillation units using surrogate column models and a support vector machine. Chem Eng Res Des 2018;134:212–25. doi:10.1016/j.cherd.2018.03.006.

[66] Deb K. Multiobjective Optimization Using Evolutionary Algorithms. New York, NY: John Wiley & Sons, Inc; 2001.

[67] Skiborowski M, Rautenberg M, Marquardt W. A Hybrid Evolutionary-Deterministic Optimization Approach for Conceptual Design. Ind Eng Chem Res 2015;54:10054–72. doi:10.1021/acs.iecr.5b01995.

[68] Institute for Energy Diversification and Saving - IDAE. Análisis del consumo energético del sector residencial en España. INFORME FINAL; 2011.

[69] U.S. Department of Energy. EnergyPlus. Energy Simulation Software: Weather Data n.d. 2015.

[70] Guadalfajara M. Evaluación de centrales solares térmicas con acumulación estacional para el sector residencial en España. 2013. doi:10.1017/CBO9781107415324.004.

[71] Jordan U, Vajen K. DHWcalc: program to generate domestic hot water profiles with statistical means for user defined conditions. Proc. ISES Sol. World Congr., Orlando (US): n.d., p. 8–12.

[72] REN21. Renewables 2020 Global Status Report. 2020.